conditions. The MS^2 spectra generated from $[M+NH_4]^+$ at *m/z* 212 showed a larger relative abundance at *m/z* 180 for MeαGlc than for MeβGlc (Fig. 4(A)). The relative abundance ratios of *m/z* 195 to 180 or *m/z* 163 to 180 were significantly different between MeαGlc and MeβGlc. The relative abundance ratios of *m/z* 195 to 180 at the different fragmentation amplitudes are shown in Fig. 4(B).

The relative abundance ratios of *m/z* 195 to 180 were more than 9 at every fragmentation amplitude for MeβGlc, but were lower than 1 for MeαGlc. The two isomers could be identified by the results in Fig. 4(B). In positive ion mode, the product ions generated from $[M+Na]^+$ at *m/z* 217 and $[M+H]^+$ or $[M+NH_4-NH_3]^+$ at *m/z* 195 showed no significant differences between α and β anomers. Therefore, the two anomers (α and β) could be distinguished from MS^2 spectra using solvent supplemented with ammonium acetate to generate $[M+NH_4]^+$ ions for analysis.

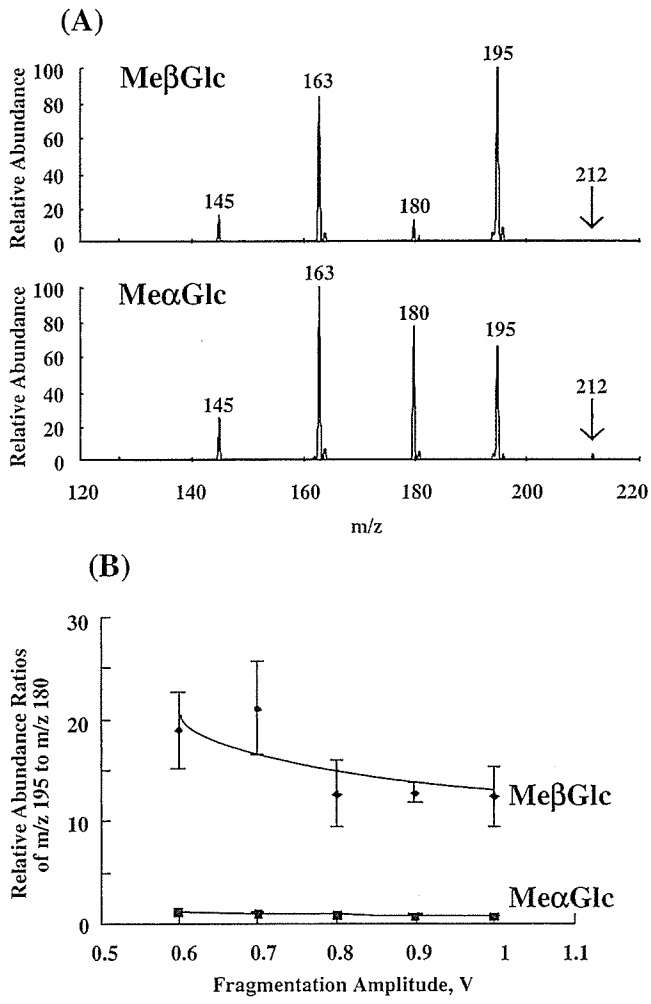

Figure 4. (A) Positive ion ESI-MS^2 spectra of MeβGlc and MeαGlc generated from precursor ion $[M+NH_4]^+$ at *m/z* 212. Fragmentation amplitude was 0.8 V. The precursor ion is indicated with a vertical arrow. (B) The relative abundance ratios of *m/z* 195 to 180 in MS^2 spectra at different fragmentation amplitudes for MeβGlc and MeαGlc. For MeαGlc, fragment ions at *m/z* 195 and 180 were detected above 0.6 V, for MeβGlc, the fragment ion at *m/z* 195 was detected above 0.5 V, and that at *m/z* 180 was detected above 0.6 V.

The mass spectra of isomers in negative ion mode were also investigated. In MS spectra, anions such as $[M+CH_3COO]^-$ at *m/z* 253 and $[M-H]^-$ at *m/z* 193 were detected for both anomers. In MS^2 spectra generated from precursor ions at *m/z* 253, a single ion species at *m/z* 193 was observed. Product ions such as $[M-CH_4O-H]^-$ at *m/z* 161, $[M-C_2H_8O_3-H]^-$ at *m/z* 113, and $[M-C_3H_8O_3-H]^-$ at *m/z* 101 were detected in MS^2 spectra generated from the precursor ion at *m/z* 193 in the MS spectrum. The base peak was *m/z* 101 for MeαGlc and *m/z* 161 for MeβGlc (Fig. 5(A)).

The relative abundance ratios of *m/z* 161 to 101 at different fragmentation amplitudes are shown in Fig. 5(B). The results showed that relative abundance ratios of *m/z* 161 to 101 were more than 2 at every fragmentation amplitude for MeβGlc,

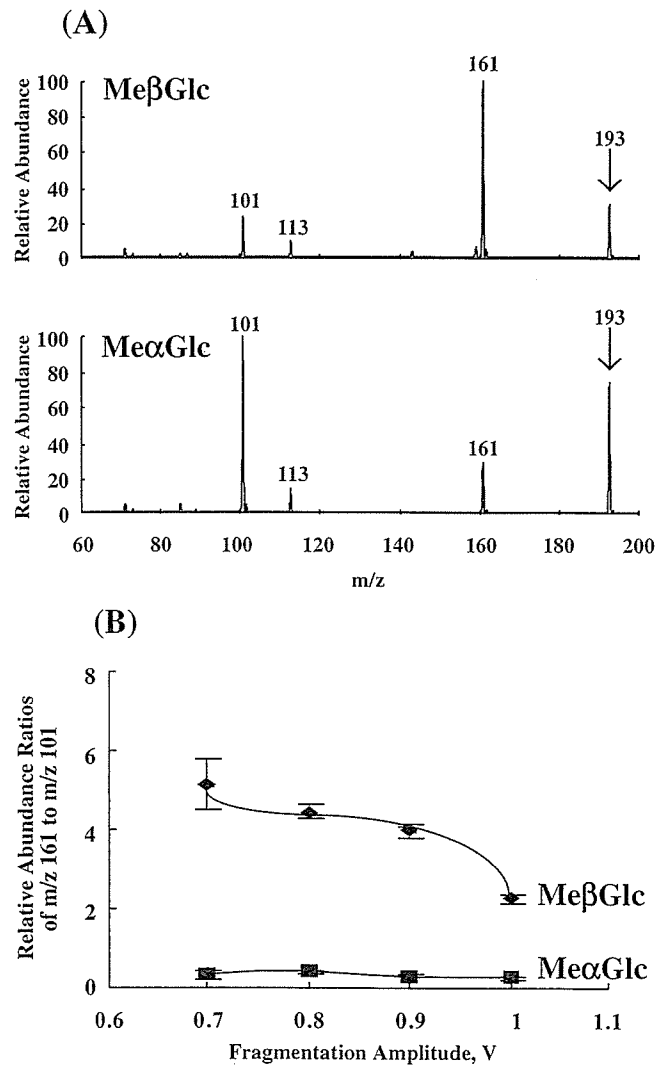

Figure 5. (A) Negative ion ESI-MS^2 spectra of MeβGlc and MeαGlc generated from precursor ion $[M-H]^-$ at *m/z* 193. Fragmentation amplitude was 0.9 V. The precursor ion is indicated with a vertical arrow. (B) The relative abundance ratios of *m/z* 161 to 101 in MS^2 spectra at different fragmentation amplitudes for MeβGlc and MeαGlc The fragment ion at *m/z* 101 was detected above 0.6 V, and that at *m/z* 161 was detected above 0.7 V for MeαGlc. The fragment ion at *m/z* 161 was observed above 0.6 V, and that at *m/z* 101 was observed above 0.7 V for MeβGlc.

DOI: 10.1002/rcm

RCM

but were lower than 0.4 for MeαGlc; the two isomers could be identified also in negative ion mode.

Therefore, MeαGlc and MeβGlc were distinguished both in positive and negative ion modes using the solvent supplemented with ammonium acetate.

Distinction between GlcN, GalN, and ManN

GlcN·HCl, GalN·HCl, and ManN·HCl in acetonitrile/water (1:1, v/v) solvent supplemented with 1 mM ammonium acetate were also examined by ESI-MS. The mass spectra showed a base peak of $[M+H]^+$ at *m/z* 180 and $[M-H_2O+H]^+$ at *m/z* 162. $[M+NH_4]^+$ at *m/z* 197 was not detected, since hexosamine with a basic NH_2 group strongly holds protons. Gas-phase basicity can be expressed in terms of gas-phase proton affinity (PA). In the gas phase, a molecule with a high gas-phase PA can abstract a proton from the protonated form of a molecule with a lower gas-phase PA.[25] The PA value of NH_3 was 204.0 kcal/mol,[26] and that of GlcN, GalN, and ManN were 223.97, 224.71, and 224.99 kcal/mol, respectively;[12] therefore, hexosamine isomers could abstract protons from NH_4^+ to produce protonated ions.

The product ion at *m/z* 162 was found in high abundance in MS^2 spectra generated from the precursor ion at *m/z* 180. MS and MS^2 spectra showed no significant differences between the three hexosamine stereoisomers; however, those isomers could be identified by the different base peaks and relative abundance in MS^3 spectra generated from the precursor ion at *m/z* 162 (Fig. 6(A)).

In the MS^3 spectra, $[M-2H_2O+H]^+$ at *m/z* 144, $[M-3H_2O+H]^+$ at *m/z* 126, and $[M-C_3H_8O_4+H]^+$ at *m/z* 72 were detected for the three isomers. $[M-C_2H_8O_4+H]^+$ at *m/z* 84 and $[C_2H_4O_2+H]^+$ at *m/z* 61 were observed in the MS^3 spectra of GlcN and ManN, and $[M-CH_8O_4+H]^+$ at *m/z* 96 was observed for GalN. The product ion that was the base peak was *m/z* 144 for GlcN, *m/z* 126 for GalN, and *m/z* 84 for ManN. Relative abundance at *m/z* 126 was larger than that at *m/z* 144 for GalN, but was lower for GlcN and ManN; therefore, GalN could be distinguished from GlcN and ManN. The product ion at *m/z* 84 showed slight relative abundance for GalN. The relative abundance of *m/z* 144 was two-fold that of *m/z* 84 for GlcN, but was almost the same for ManN; therefore, GlcN could be distinguished from ManN. Furthermore, MS^3 spectra were measured by altering fragmentation amplitudes from 0.4 through 1.0 V (Fig. 6(B)).

Since the relative abundance ratios of *m/z* 144 to 126 were 0.3–0.45 for GalN, 1–3 for ManN, and 2–5 for GlcN, GalN could be distinguished from GlcN and ManN. Moreover, GlcN and ManN were identified by relative abundance ratios

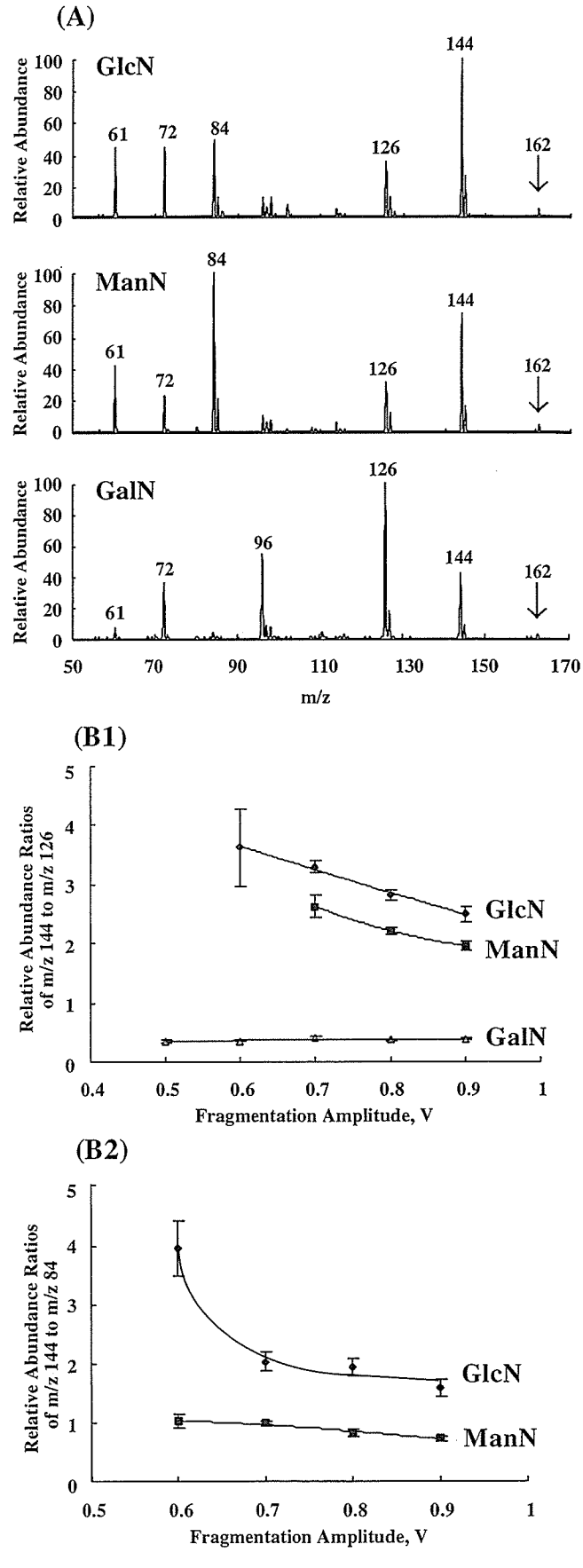

Figure 6. (A) Positive ion ESI-MS^3 spectra of GlcN, ManN, and GalN generated from precursor ion $[M-H_2O+H]^+$ at *m/z* 162. Fragmentation amplitude was 0.8 V. The precursor ion is indicated with a vertical arrow. The relative abundance ratios of (B1) *m/z* 144 to 126 and (B2) *m/z* 144 to *m/z* 84 in MS^3 spectra at different fragmentation amplitudes for GlcN, ManN, and GalN. The fragment ion at *m/z* 144 was detected above 0.5 V for GlcN and GalN, and above 0.6 V for ManN. The fragment ion at *m/z* 126 was detected above 0.5 V for GalN, 0.6 V for GlcN, and 0.7 V for ManN. The fragment ion at *m/z* 84 was detected above 0.6 V for GlcN and ManN, but not for GalN.

DOI: 10.1002/rcm

of *m/z* 144 to 84 of 0.5–1 for ManN and 1.5–5 for GlcN; therefore, distinctions between the three $HexNH_2$ isomers were possible in the presence of ammonium acetate.

Distinction between GlcNAc, GalNAc, and ManNAc

MS^n spectra of GlcNAc, GalNAc, and ManNAc were investigated using solvent supplemented with ammonium acetate in positive ion mode. In MS spectra, $[M+H]^+$ at *m/z* 222 was observed for the three isomers. Simultaneously, in-source fragment ions such as $[M-H_2O+H]^+$ at *m/z* 204 and $[M-2H_2O+H]^+$ at *m/z* 186 were detected. The abundance of $[M+NH_4]^+$ at *m/z* 239 was too low to measure MS^2 spectra. The abundance of $[M+H]^+$ at *m/z* 222 showed a marked increase by the addition of ammonium acetate. The PA values of GlcNAc, GalNAc, and ManNAc were 221.1, 221.6, and 221.2 kcal/mol, respectively.[14] Since the gas-phase basicity of *N*-acetylhexosamines as well as hexosamines was higher than that of NH_3, *N*-acetylhexosamines could abstract protons from NH_4^+ to produce protonated ions.

In MS^2 spectra, product ions such as $[M-H_2O+H]^+$at *m/z* 204, $[M-2H_2O+H]^+$ at *m/z* 186, and $[M-C_2H_8O_4+H]^+$ at *m/z* 126 were generated from $[M+H]^+$ at *m/z* 222; however, they showed no significant difference in relative abundance (data not shown).

In MS^3 spectra (Fig. 7(A)), many product ions were observed when $[M-H_2O+H]^+$ at *m/z* 204 was a precursor ion. Product ions such as $[M-2H_2O+H]^+$ at *m/z* 186, $[M-3H_2O+H]^+$ at *m/z* 168, $[M-C_2H_6O_3+H]^+$ at *m/z* 144, $[M-CH_8O_4+H]^+$ at *m/z* 138, $[M-C_2H_8O_4+H]^+$ at *m/z* 126, and $[M-C_4H_{10}O_5+H]^+$ at *m/z* 84 were detected for the three isomers. The product ion base peak was *m/z* 126 for ManNAc and *m/z* 186 for GlcNAc and GalNAc. The relative abundance of *m/z* 126 was larger than that of *m/z* 186 for ManNAc, but was lower for GlcNAc and GalNAc; therefore, ManNAc could be distinguished from GlcNAc and GalNAc. The relative abundance of *m/z* 126 was larger than that of *m/z* 168 for GalNAc, but was lower for GlcNAc; thus, GlcNAc and GalNAc could also be distinguished from each other. Furthermore, MS^3 spectra were measured by altering fragmentation amplitudes from 0.5 through 1.1 V (Fig. 7(B)).

The relative abundance ratios of *m/z* 186 to 126 were larger than 1 for GlcNAc and GalNAc, and were lower than 1 for ManNAc (Fig. 7(B1)), while the relative abundance ratios of *m/z* 168 to 126 were larger than 1.5 for GlcNAc, and were lower than 0.3 for GalNAc and ManNAc (Fig. 7(B2)); therefore, distinctions between the three HexNAc isomers were possible in the presence of ammonium acetate.

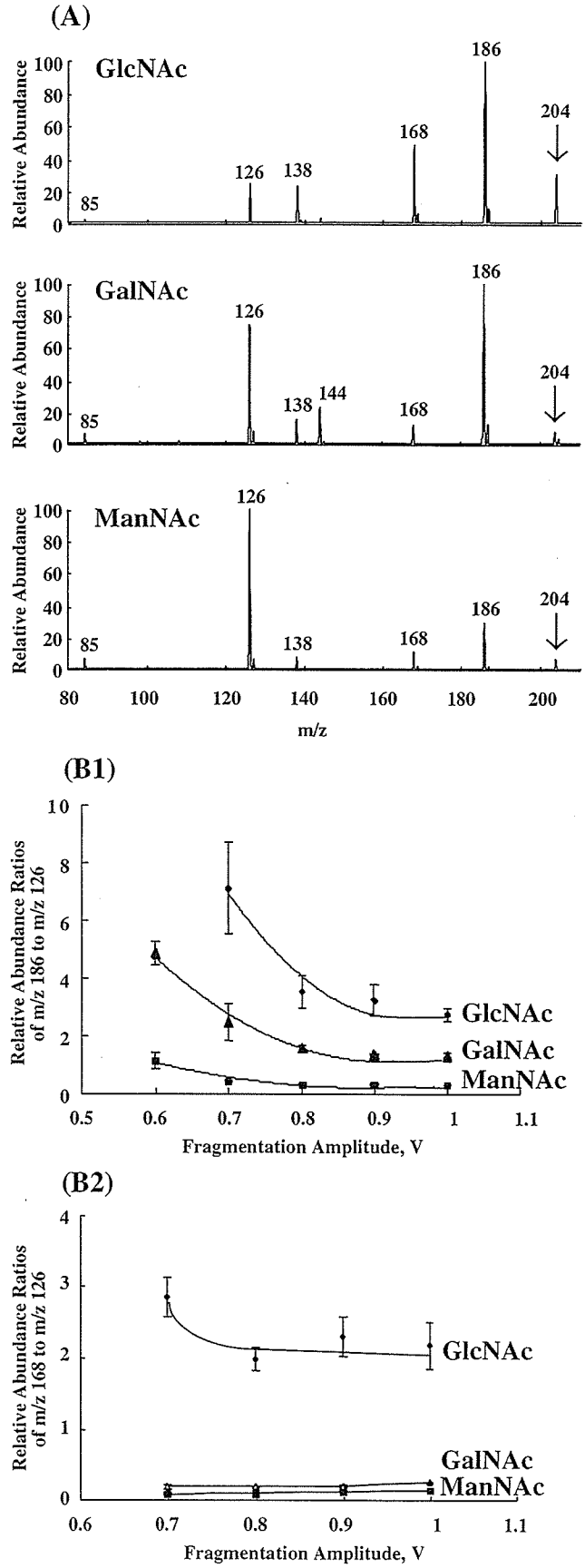

Figure 7. (A) Positive ion ESI-MS^3 spectra of GlcNAc, GalNAc and ManNAc generated from precursor ion $[M-H_2O+H]^+$ at *m/z* 204. Fragmentation amplitude is 0.8 V. The precursor ion is indicated with a vertical arrow. The relative abundance ratios of (B1) *m/z* 186 to 126 and (B2) *m/z* 168 to 126 in MS^3 spectra at the different fragmentation amplitudes for GlcNAc, GalNAc, and ManNAc. The fragment ion at *m/z* 186 was detected above 0.5 V for ManNAc, and 0.6 V for GlcNAc and GalNAc. The fragment ion at *m/z* 168 was detected above 0.6 V for GlcNAc, and 0.7 V for GalNAc and ManNAc. The fragment ion at *m/z* 126 was detected above 0.6 V for GalNAc and ManNAc, and 0.7 V for GlcNAc.

DOI: 10.1002/rcm

RCM

Next, MS^2 and MS^3 spectra of $[M+Na]^+$ at *m/z* 244 produced using solvent supplemented with 10 μM sodium acetate were examined. In MS^2 spectra, $[M-H_2O+Na]^+$ at *m/z* 226 was observed for the three isomers. The MS^3 spectra generated from *m/z* 226 showed several product ions including $[M-CH_4O_2+Na]^+$ at *m/z* 196, $[M-C_2H_5O_3+Na]^+$ at *m/z* 167, and $[M-C_2H_8O_4+Na]^+$ at *m/z* 148; however, GlcNAc and ManNAc could not be distinguished from the MS^3 spectra. Therefore, use of the Na^+-adducted ion as a precursor ion was inappropriate to distinguish between GlcNAc, GalNAc, and ManNAc.

CONCLUSIONS

In conclusion, we found a new method for distinguishing Glc, Gal and Man using $[M+NH_4]^+$ ions generated in solutions of acetonitrile/water (1:1, v/v) solvent supplemented with 1 mM ammonium acetate by ESI-ITMS. Glc was distinguished from Gal and Man in MS^2 spectra, while Gal and Man were distinguished by MS^3 analyses. The anomeric isomers of MeαGlc and MeβGlc could also be identified using MS^2 spectra of $[M+NH_4]^+$ ions. The $HexNH_2$ isomers (GlcN, GalN, and ManN) and HexNAc isomers (GlcNAc, GalNAc, and ManNAc) could also be distinguished by measuring MS^3 spectra using the same solvent. The measurement of relative abundance ratios of the characteristic fragment ions in MS^2 and MS^3 spectra depending on the collision energy gave very credible results for the distinction of monosaccharide isomers. Therefore, the acetonitrile/water (1:1, v/v) solvent supplemented with 1 mM ammonium acetate was a common solvent for distinguishing monosaccharide isomers by ESI-ITMS. We would like to apply this method for the sequence analyses of oligosaccharides and mixtures of monosaccharides in the future.

Acknowledgements

The authors are grateful to Dr. Peixing Wu for fruitful discussions concerning these experiments. This study was partly supported through Special Coordination Funds for Promoting Science and Technology from the Ministry of Education, Culture, Sports, Science and Technology, the Japanese Government.

REFERENCES

1. Variki A. *Glycobiology* 1993; **3**: 97. DOI: 10.1093/glycob/3.2.97.
2. Chaplin MF, Kennedy JF (eds). *Carbohydrate Analysis: A Practical Approach* (2nd edn). Oxford University Press: USA, 1994.
3. Gaucher SP, Leary JA. *Anal. Chem.* 1998; **70**: 3009. DOI: 10.1021/ac980023k.
4. Chaplin MF, Kennedy JF (eds). *Carbohydrate Analysis: A Practical Approach*. IRL Press: Oxford, 1986.
5. Mechref Y, Novotny MV. *Chem. Rev.* 2002; **102**: 321. DOI: 10.1021/cr0103017.
6. Zaia J. *Mass Spectrom. Rev.* 2004; **23**: 161. DOI: 10.1002/mas.10073.
7. Cuyckens F, Shahat AA, Pieters L, Claeys M. *J. Mass Spectrom.* 2002; **37**: 1272. DOI: 10.1002/jms.402.
8. Desaire H, Leary JA. *Anal. Chem.* 1999; **71**: 4142. DOI: 10.1021/ac990553w.
9. Salpin JY, Tortajada J. *J. Mass Spectrom.* 2002; **37**: 379. DOI: 10.1002/jms.289.
10. Smith G, Leary JA. *J. Am. Chem. Soc.* 1996; **118**: 3293. DOI: 10.1021/ja952915x.
11. Smith G, Pedersen SF, Leary JA. *J. Org. Chem.* 1997; **62**: 2152. DOI: 10.1021/jo9622789.
12. Nagaveni V, Prabhakar S, Vairamani M. *Anal. Chem.* 2004; **76**: 3505. DOI: 10.1021/ac049829c.
13. Young MK, Dinh N, Williams D. *Rapid Commun. Mass Spectrom.* 2000; **14**: 1462. DOI: 10.1002/1097-0231(20000830)14:16<1462::AID-RCM48>3.0.CO;2-Y.
14. Nagaveni V, Vairamani M. *Rapid Commun. Mass Spectrom.* 2003; **17**: 1089. DOI:10.1002/rcm.1018.
15. Desaire H, Leary JA. *Anal. Chem.* 1999; **71**: 1997. DOI: 10.1021/ac981052y.
16. Desaire H, Leary JA. *J. Am. Soc. Mass Spectrom.* 2000; **11**: 1086. DOI:10.1016/S1044-0305(00)00179-3.
17. Cancilla MT, Penn SG, Carroll JA, Lebrilla CB. *J. Am. Chem. Soc.* 1996; **118**: 6736. DOI: 10.1021/ja9603766.
18. Zamfir A, Peter-Katakinic J. *Electrophoresis* 2004; **25**: 1949. DOI: 10.1002/elps.200405825.
19. March RE, Stadey CJ. *Rapid Commun. Mass Spectrom.* 2005; **19**: 805. DOI:10.1002/rcm.1860.
20. Taylor VF, March RE, Longerich HP, Stadey CJ. *Int. J. Mass Spectrom.* 2005; **243**: 71. DOI:10.1016/j.ijms.2005.01.001.
21. March RE, Lewars EG, Stadey CJ, Maio XS, Zhao XM, Metcalfe CD. *Int. J. Mass Spectrom.* 2006; **248**: 61. DOI: 10.1016/j.ijms.2005.09.011.
22. Hogg AM, Nagabhushan TL. *Tetrahedron Lett.* 1972; **13**: 4827. DOI: 10.1016/S0040-4039(01). 94440–5.
23. Denekamp C, Sandlers Y. *J. Mass Spectrom.* 2005; **40**: 765. DOI: 10.1002/jms.848.
24. Carroll JA, Willard D, Lebrilla CB. *Analytica Chimica Acta* 1995; **307**: 431. DOI:10.1016/0003-2670(94)00514-M.
25. Cesh NB, Enke CG. *Mass Spectrom. Rev.* 2001; **20**: 362. DOI: 10.1002/mas.10008.
26. Data from NIST Standard Reference Database 69, June 2005 Release: NIST Chemistry WebBook. Available: http://webbook.nist.gov./chemistry/

ELSEVIER

EXPERIMENTAL HEMATOLOGY

Experimental Hematology 34 (2006) 508–518

Involvement of insulin-like growth factor-I and insulin-like growth factor binding proteins in pro–B-cell development

Tomoko Taguchi[a,b], Hisami Takenouchi[a], Jun Matsui[a], Wei-Ran Tang[a], Mitsuko Itagaki[a], Yusuke Shiozawa[a], Kyoko Suzuki[a], Sachi Sakaguchi[a], Yohko U. Ktagiri[a], Takao Takahashi[b], Hajime Okita[a], Junichiro Fujimoto[a], and Nobutaka Kiyokawa[a]

[a]*Department of Developmental Biology, National Research Institute for Child Health and Development, Setagaya-ku, Tokyo;* [b]*Department of Pediatrics, Keio University, School of Medicine, Shinjuku-ku, Tokyo, Japan*

(Received 14 March 2005; revised 12 December 2005; accepted 12 January 2006)

Objective. **Insulin-like growth factor (IGF)-binding proteins (IGFBPs) are a family of proteins thought to modulate IGF function. By employing an in vitro culture system of human hematopoietic stem cells cocultured with murine bone marrow stromal cells, we examined the effects of IGF-I and IGFBPs on early B-cell development.**

Materials and Methods. **Human CD34$^+$ bone marrow cells were cocultured with murine stromal MS-5 cells for 4 weeks, and pro–B-cell number was analyzed by flow cytometry. After administration of reagents that are supposed to modulate IGF-I or IGFBP function to the culture, the effect on pro–B-cell development was examined.**

Results. **After cultivation for 4 weeks, effective induction of pro–B-cell proliferation was observed. Experiments using several distinct factors, all of which neutralize IGF-I function, revealed that impairment of IGF-I function results in a significant reduction in pro–B-cell development from CD34$^+$ cells. In addition, when the effect of recombinant proteins of IGFBPs and antibodies against IGFBPs were tested, IGFBP-3 was found to inhibit pro–B-cell development, while IGFBP-6 was required for pro–B-cell development.**

Conclusions. **IGF-I is essential for development of bone marrow CD34$^+$ cells into pro-B cells. Moreover, IGFBPs are likely involved in regulation of pro–B-cell development.** © **2006 International Society for Experimental Hematology. Published by Elsevier Inc.**

Insulin-like growth factor-I (IGF-I) is an anabolic hormone and, like growth hormone and insulin, regulates whole body growth, metabolism, tissue repair, and cell survival [1]. In addition to its main production by the liver, IGF-I is also produced by bone marrow (BM) stromal cells, myeloid cells, and peripheral lymphocytes. In plasma and most biological fluids, IGF-I binds to members of a family of six specific soluble proteins, known as IGF-binding proteins (IGFBPs) 1–6, all of which have structures that are unrelated to those of IGF receptors (IGFRs) [2]. Although IGFBPs were originally described as passive circulating transport proteins, they are now recognized as playing a variety of roles in circulation, the extracellular environment, and inside the cell [3,4].

Offprint requests to: Tomoko Taguchi, M.D., Ph.D., Department of Developmental Biology, National Research Institute for Child Health and Development, 2-10-1, Okura, Setagaya-ku, Tokyo 154-8535, Japan; E-mail: ttaguchi@nch.go.jp

Of the six IGFBPs, IGFBP-3 is the most abundant IGFBP in plasma. In vitro experiments examining the effects of IGFBP-3 on various cell cultures have provided conflicting data, with both enhancement and inhibition of IGF-I actions, depending upon the cell type and culture conditions used [3,4]. In contrast, IGFBP-6 was purified from human cerebrospinal fluid and from transformed human fibroblast cell culture [3]. IGFBP-6 has been shown to inhibit IGF actions, including proliferation, differentiation, cell adhesion, and colony formation of osteoblasts and myoblasts [4]. Although the IGFBPs differ in their structure and binding specificity, functional differences among the various IGFBPs are still not clear [4].

In view of its multiple effects, IGF-I is thought to play an integral role in hematopoiesis [1]. IGF-I stimulates growth of bones and seems to control the volume of BM, thereby regulating production of hematopoietic cells [5]. Moreover, IGF-I has been suggested to have direct effects on development of a variety of hematopoietic cells. In the case of

0301-472X/06 $–see front matter.
doi: 10.1016/j.exphem.2006.01.009

B-cell development in mice, for example, previous reports have indicated that IGF-I stimulates maturation of pro-B cells into pre-B cells [6] and acts as a B-cell proliferation cofactor to synergize with the activity of interleukin (IL)-7 [7]. Indeed, administration of IGF-I increased the number of pre-B cells in BM and splenic B cells in normal mice and after BM transplantation [8]. However, the effect of IGF-I on B-cell development, especially in humans, is still largely unknown. In addition, although murine BM stromal cells secrete IGFBPs, the functional role of them in hematopoiesis remains unclear.

In an attempt to clarify the effect of IGF-I and IGFBPs on early B-cell development, we employed an in vitro culture system of human hematopoietic stem cells (HPSCs) cocultured with murine BM stromal cells that induce pro-B cells. In this article, we expand upon results of previous reports by other authors [6–8] and show that IGF-I is essential for pro–B-cell induction from HPSCs. In addition, we also report that IGFBP-3 inhibits pro–B-cell development, whereas IGFBP-6 is required for pro–B-cell development. The possible role of IGFBPs in early B-cell development is discussed.

Materials and methods

Reagents

Recombinant human and mouse IGF-I, IGFBPs, and the IGF-IR kinase inhibitor I-OMe-AG538 were obtained from PeproTech EC Ltd. (London, UK), G-T Research Products (Minneapolis, MN, USA), and Calbiochem-Novabiochem Co. (San Diego, CA, USA), respectively. All reagents are solved in phosphate-buffered saline, except I-Ome-AG538, which is solved in dimethyl sulfoxide, and diluted to the indicated concentration by culture medium.

The following mouse monoclonal antibodies (mAbs) against human antigens were used: anti-IGF-IR from G-T; purified anti-CD19, fluorescein isothiocyanate (FITC)-conjugated anti-μ heavy chain, and phycoerythrin (PE)-conjugated anti-κ and anti-λ light chains and anti-CD25 from Becton Dickinson Biosciences (San Diego, CA, USA); FITC-conjugated anti-CD24, CD43, and CD45, PE-conjugated anti-CD10, CD20, CD33, and CD179a, and PE-cyanine (PC)-5–conjugated anti-CD19 from Beckman/Coulter Inc. (Westbrook, MA, USA). The CD179a molecule, also known as VpreB, is a component of surrogate light chain and is specifically expressed in B-cell precursors, including pro-B and pre-B cells, but not in mature B cells [9]. Hamster mAb against mouse IGF-I and goat polyclonal anti-mouse IGF-I, and IGFBPs Abs were obtained from G-T. Rabbit polyclonal Abs against human IGF-IR and phosphospecific IGF-IR were purchased from Cell Signaling Technology (Beverly, MA, USA). Goat polyclonal anti–β-actin Ab was obtained from Santa Cruz Biotechnology, Inc. (Santa Cruz, CA, USA). Secondary Abs were obtained from Molecular Probes, Inc. (Eugene, OR, USA), and Dako Cytomation, Co. (Glostrup, Denmark), respectively. All other chemical reagents were obtained from Wako Pure Chemical Industries, Ltd. (Osaka, Japan), unless otherwise indicated.

Cells and cultures

Human BM $CD34^+$ cells purchased from Cambrex Bio Science Walkersville, Inc. (Walkersville, MD, USA) were used. These cells had been isolated from human tissue after obtaining informed consent. A cloned murine BM stromal cell line, MS-5, was kindly provided by Dr. A. Manabe (St. Luke's International Hospital, Tokyo, Japan) and Dr. K. J. Mori (Nigata University, Nigata, Japan). Human B-precursor acute lymphoblastic leukemia cell line NALM-16 was kindly provided by Dr. Y. Matsuo (Grand Saule Immuno research Laboratory, Nara, Japan) and was maintained in RPMI-1640 supplemented with 10% (v/v) fetal calf serum (FCS; Sigma-Aldrich Fine Chemical Co., St. Louis, MO, USA) at 37°C in a humidified 5% CO_2 atmosphere.

For induction of pro-B cells, MS-5 cells were plated at a concentration of 1×10^5 cells on a 12-well tissue plate (Asahi Techno Glass Co., Chiba, Japan). The next day, 4×10^4 cells/well/2 mL $CD34^+$ cells were plated onto the MS-5 cells in culture medium supplemented with 10% FCS and various combinations of reagents, as indicated in the figures. Because our preliminary experiments revealed that cultures in an RPMI-1640 medium produced a higher yield of B cells compared with cultures in α-minimum essential medium (data not shown), we used RPMI-1640 medium for the following experiments. After cultivation for the indicated periods, cells were harvested using 0.25% trypsin plus 0.02% ethylenediamine tetraacetic acid (IBL Co. Ltd., Gunma, Japan), and the number of cells per well was determined. All experiments were performed in triplicate, and means ± standard deviations (SD) of cell numbers are shown in Figures 1C, 3, 4, 5C, and 5D. For the histology studies, cells were cultured on type-I collagen-coated cover slips (Asahi Techno Glass) and were examined by May-Grünwald-Giemsa staining or immunohistochemical staining.

Immunofluorescence study

A multicolor immunofluorescence study was performed using a combination of FITC, PE, and PC-5. Cells were stained with fluorescence-labeled mAbs and analyzed by flow cytometry (EPICS-XL, Beckman/Coulter), as described previously [10]. Staining of the cytoplasmic antigens was performed using Cytofix/Cytoperm Kits (Becton Dickinson), according to manufacturer's protocol. To detect surface immunoglobulin $(Ig)^+$ mature B cells and cytoplasmic μ^+ pre-B cells simultaneously, cells were first stained with a mixture of PC-5-conjugated anti-CD19 Ab and PE-conjugated Abs against κ/λ light chains and then treated with cell permeabilization reagents followed by staining of cytoplasmic antigens. It was confirmed by preliminary experiments that permeabilization treatment does not affect the signals of surface antigens stained beforehand. For cell sorting, human BM $CD34^+$ cells cocultured with MS-5 for 4 weeks were harvested and stained with PC-5–conjugated anti-CD19 mAb. $CD19^+$ cells were sorted in an EPICS-ALTRA cell sorter (Beckman/Coulter). For CD19 immunostaining, cover slips were fixed with ice-cold acetone for 15 minutes and stained with anti-CD19 mAb and examined by confocal laser scanning microscope (FV500; Olympus, Tokyo, Japan) as described previously [11].

RT-PCR, immunoblotting, and detection of IGF-I

Total RNA was extracted from cultured cells, and reverse transcriptase polymerase chain reaction (RT-PCR) was performed as described previously [12]. The sets of primers used in this study are listed in Table 1. Cell lysates were prepared by solubilizing the cells in lysis buffer and immunoblotting was performed as described previously [13]. The concentration of mouse IGF-I in

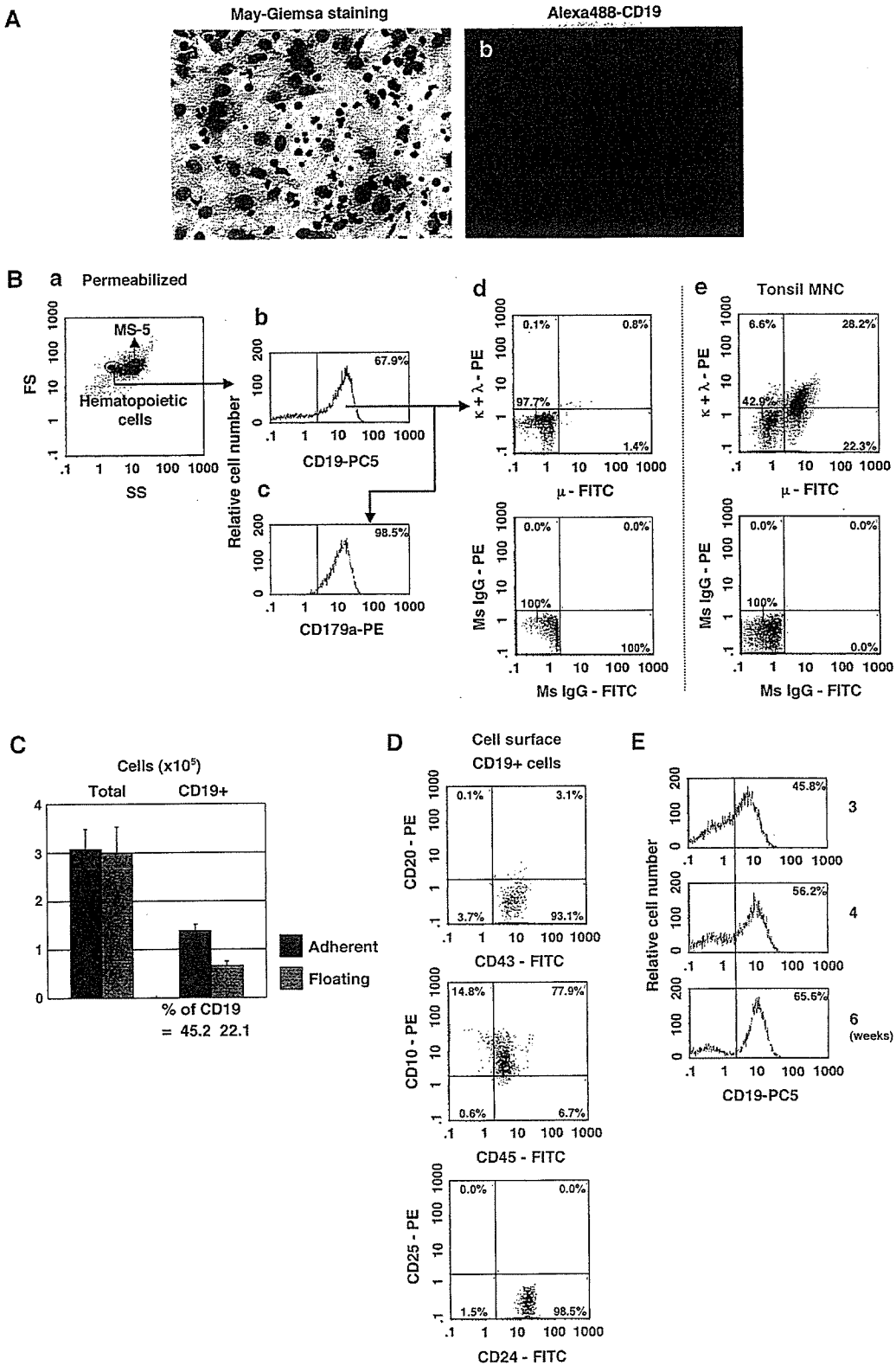
A
May-Giemsa staining
Alexa488-CD19
b
B a Permeabilized
MS-5
Hematopoietic cells
FS
SS
b
67.9%
CD19-PC5
Relative cell number
c
98.5%
CD179a-PE
d
0.1%
0.8%
97.7%
1.4%
κ + λ - PE
μ - FITC
0.0%
0.0%
100%
100%
Ms IgG - PE
Ms IgG - FITC
e
Tonsil MNC
6.6%
28.2%
42.9%
22.3%
0.0%
0.0%
100%
0.0%
C
Cells (x10⁵)
Total
CD19+
Adherent
Floating
% of CD19
= 45.2 22.1
D
Cell surface
CD19+ cells
0.1%
3.1%
3.7%
93.1%
CD20 - PE
CD43 - FITC
14.8%
77.9%
0.6%
6.7%
CD10 - PE
CD45 - FITC
0.0%
0.0%
1.5%
98.5%
CD25 - PE
CD24 - FITC
E
45.8%
3
56.2%
4
65.6%
6
(weeks)
Relative cell number
CD19-PC5

culture supernatants of MS-5 cells was determined by sandwich enzyme-linked immunosorbent assay (ELISA), using Mouse IGF-I Quantikine ELISA Kit (R&D Systems, Wiesbaden, Germany), according to manufacturer's instruction. Experiments were performed in triplicate, and mean ± SDs of cell numbers are shown in Figure 2C.

Results

Differentiation of pro-B cells from human BM CD34$^+$ cells by coculturing with murine stromal MS-5 cells

Murine stromal cell line MS-5 has been reported to possess the capability to support differentiation of B-lineage cells from human cord blood (CB) CD34$^+$ cells [14–17]. Coincident with these previous reports, we observed that human BM CD34$^+$ cells generated a high number of CD19$^+$ B cells after cocultivation with MS-5 cells (Fig. 1A and B). Starting with 4×10^4 CD34$^+$ cells, approximately 0.4 to 1.3×10^6 mononuclear cells, 30.1% to 68.2% of which were CD19$^+$ cells, were obtained after 4 weeks of cultivation. As shown in Figure 1C, approximately half of the hematopoietic cells were floating, while the remainder were adhered to the MS-5 cells and the CD19$^+$ cells were more abundant in adherent cell fraction.

As shown in Figure 1B, most of the CD19$^+$ B cells obtained after 9 weeks of cultivation expressed cytoplasmic CD179a. The CD179a is reported to be already expressed in pro-B cells, remains expressed on B-cell precursors, and disappears upon differentiation from pre-B cells to mature B cells [9]. In contrast, a few percent of CD19$^+$ cells were positive for surface and/or cytoplasmic μ heavy chain and a portion of them expressed either the κ or λ light chains (Fig. 1B). We also observed that CD10, CD24, CD43, and CD45 were expressed but CD20 and CD25 were not in the CD19$^+$ cells (Fig. 1D). No difference in immunophenotypic characteristics was observed between the CD19$^+$ cells in adherent cell fraction and that in floating cell fraction (data not shown). Based on the above data, we concluded that human BM CD34$^+$ cells can differentiate into pro-B cells, but not into pre-B cells, after coculturing with the murine stromal cell line MS-5 in the present culture system. CD19$^+$ cells cultured for 4 weeks were also examined, and similar immunophenotypic characteristics were noted (data not shown).

Next, we examined the time course of the expression of CD19 in human BM CD34$^+$ cells in our culture system. CD19$^+$ cells were already detected after 1 week of culture (data not shown), and the number of CD19$^+$ cells increased throughout the course of the cell culture thereafter. After 4 to 9 weeks of culture, both the fluorescent intensity of CD19 on each cell and the percentage of CD19$^+$ cells out of the total number of cells continued to increase (Fig. 1E), but the total number of CD19$^+$ cells did not change significantly (data not shown). When expression of transcription factors related to early B-cell differentiation was analyzed by RT-PCR, expression profiles of these factors were well correlated with proliferation of CD19$^+$ cells as described (data not shown). Therefore, pro–B-cell development after 4 weeks of culture in the present system was analyzed in the following experiments.

Effect of IGF-I on in vitro human pro–B-cell development

Because expression of IGFRs in cultured CD34$^+$ BM cells was detected (Fig. 2A), we first tested the effect of adding exogenous recombinant human IGF-I to the coculture of CD34$^+$ BM cells and MS-5 cells to evaluate the contribution of IGF-I to human pro–B-cell development; no significant change in pro–B-cell development was observed (data not shown).

However, RT-PCR analysis revealed expression of IGF-I in MS-5 cells (Fig. 2B). Results of ELISA further demonstrated that mouse IGF-I was indeed secreted in the culture supernatant of MS-5 cells (Fig. 2C). As presented in Figure 2D, mouse IGF-I is active in human hematopoietic cells and can induce tyrosine-phosphorylation of human IGF-IR expressed on NALM-16 cells derived from human B-precursor acute lymphoblastic leukemia. When we tested similarly, MS-5 culture supernatant could stimulate IGF-IR on NALM-16 cells, whereas freshly prepared medium containing 10% FCS could not, indicating that mouse IGF-I secreted from MS-5 cells is sufficient to stimulate

Figure 1. Characterization of human bone marrow (BM) CD34$^+$ cells cocultured with murine stromal cells. (**A**) Human BM CD34$^+$ cells were cocultured for 4 weeks with murine stromal MS-5 cells on cover slips. At the end of the culture period, the cells were examined with either May-Grünwald-Giemsa staining (**a**) or CD19 immunostaining (green) with nuclear counter staining by 4′,6-diamidino-2-phenylindole (blue) (**b**). Original magnification ×400. (**B**) Human BM CD34$^+$ cells cocultured for 9 weeks with MS-5 cells were harvested. The expression of cell surface CD19, κ/λ light chains and cytoplasmic CD179a and μ heavy chain was simultaneously assessed by flow cytometry with cell-permeabilization technique as described in Materials and Methods. In cultured BM cells (**a**), CD19$^+$ cells were gated (**b**), and expression of CD179a (**c**), μ heavy chain, and κ/λ light chains (**d**) was examined. As a negative control, same sample specimen stained with isotype-matched control mouse IgG was also presented. As a positive control, mononuclear cells prepared from tonsil were similarly treated as in (**d**) and presented (**e**). FITC = fluorescein isothiocyanate; FS = forward light scatter; SS = side light scatter. (**C**) Human BM CD34$^+$ cells were cocultured with MS-5 cells for 4 weeks and the adherent cell fraction and floating cell fraction were collected separately. Total cell number and expression of CD19 were examined as above. (**D**) Human BM CD34$^+$ cells were cocultured with MS-5 cells as in (**B**), and multicolor immunofluorescence study was performed as above. CD19$^+$ cells were gated, and expression of surface B-cell differentiation markers, as indicated, was examined using flow cytometry. (**E**) Human BM CD34$^+$ cells were cocultured with MS-5 cells for 3, 4, and 6 weeks, and expression of CD19 was examined using flow cytometry.

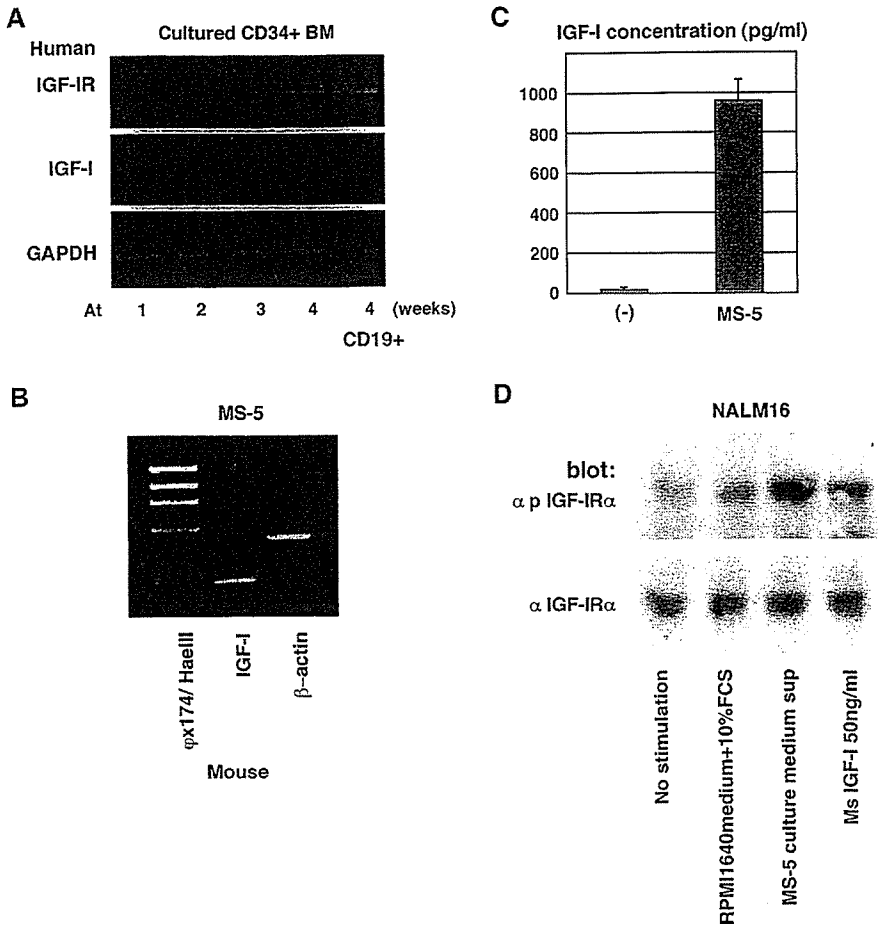

Figure 2. Expression of insulin-like growth factors (IGFs) and IGF receptors on cultured human bone marrow (BM) $CD34^+$ cells and murine stromal MS-5 cells. (**A**) Human BM $CD34^+$ cells were cocultured with MS-5 cells for 1, 2, 3, or 4 weeks, as shown in Figure 1. At the end of the culture periods, the floating fraction of the cultured human BM cells was collected and expression of human IGF-I receptor (IGF-IR) and IGF-I was examined using reverse transcriptase polymerase chain reaction (RT-PCR). As an internal control, expression of human glyceraldehyde phosphate dehydrogenase was also examined. $CD19^+$ cells were sorted from 4-week cultured human BM $CD34^+$ cells and similarly examined ($CD19^+$). (**B**) Expression of mouse IGF-I in MS-5 cells was examined using RT-PCR. As an internal control, expression of mouse β-actin was also examined. The $\phi\chi174$/*Hae*III molecular weight marker was presented in the left side. (**C**) MS-5 cells were cultured alone for 4 weeks and the culture supernatant was collected. Subsequent concentration of mouse IGF-I secreted by MS-5 cells in culture supernatant was determined by enzyme-linked immunosorbent assay. As a negative control, freshly prepared medium containing 10% fetal calf serum (FCS) was also examined, and no significant crossreaction was observed. (**D**) Biological effect of mouse IGF-I secreted by MS-5 cells on human hematopoietic cells was examined using NALM-16 cells that express IGF-IR. Cells at logarithmic growth were stimulated for 5 minutes with either freshly prepared culture medium containing 10% FCS, MS-5 culture supernatant, or recombinant mouse IGF-I (final concentration at 50 ng/mL) and examined by immunoblotting using antiphosphospecific human IGF-IR Ab that only recognize the activated form of IGF-IR. As a control, anti-entire IGF-IR Ab was also used.

human hematopoietic cells. Therefore, the data suggest a possibility that MS-5 cells secrete excess amounts of IGF-I and thus exogenous addition of recombinant IGF-I revealed no effect on pro–B-cell development.

Indeed, when anti-mouse IGF-I Ab, which neutralizes the effect of IGF-I, was added to the culture, development of $CD19^+$ B cells was significantly reduced (Fig. 3A and B). As shown in Figure 3B, the initial addition of 5 μg/mL polyclonal goat anti-mouse IGF-I Ab was sufficient to induce a significant reduction in pro–B-cell development. When hamster anti-mouse IGF-I mAb was used, however, additional Abs were required to produce a remarkable reduction in subsequent pro–B-cell production (Fig. 3A). In both cases, anti-mouse IGF-I Abs not only reduced the total cell number of cultured $CD34^+$ BM cells, but also remarkably diminished the percentage of $CD19^+$ B cells out of the total number of cells in the culture. Therefore, reduction in $CD19^+$ B cells is not merely the result of an overall cell reduction. Moreover, anti-mouse IGF-I Ab-induced reduction in $CD19^+$ B-cell development was cancelled by the addition of recombinant human IGF-I (Fig. 3D). The data suggests that IGF-I significantly participates in pro–B-cell development. Evidence that anti-human IGF-IR Ab and IGF-IR kinase inhibitor, both of which can block the effect of IGF-I, reduce pro–B-cell development, further supports this notion (Fig. 3B and C).

Of note, RT-PCR analysis also showed a time-dependent expression of IGF-I in a total cell fraction, but not sorted $CD19^+$ cell fraction, of the cultured human BM $CD34^+$ cells during the culture period (Fig. 2A). Beside $CD19^+$ cell fraction, $CD33^+$ myelomonocytic cells were present in the culture (data not shown). Although $CD33^+$ cell population was decreasing with the culture time, they matured with time. Thus, time-dependent expression of IGF-I is most likely due to this cell fraction.

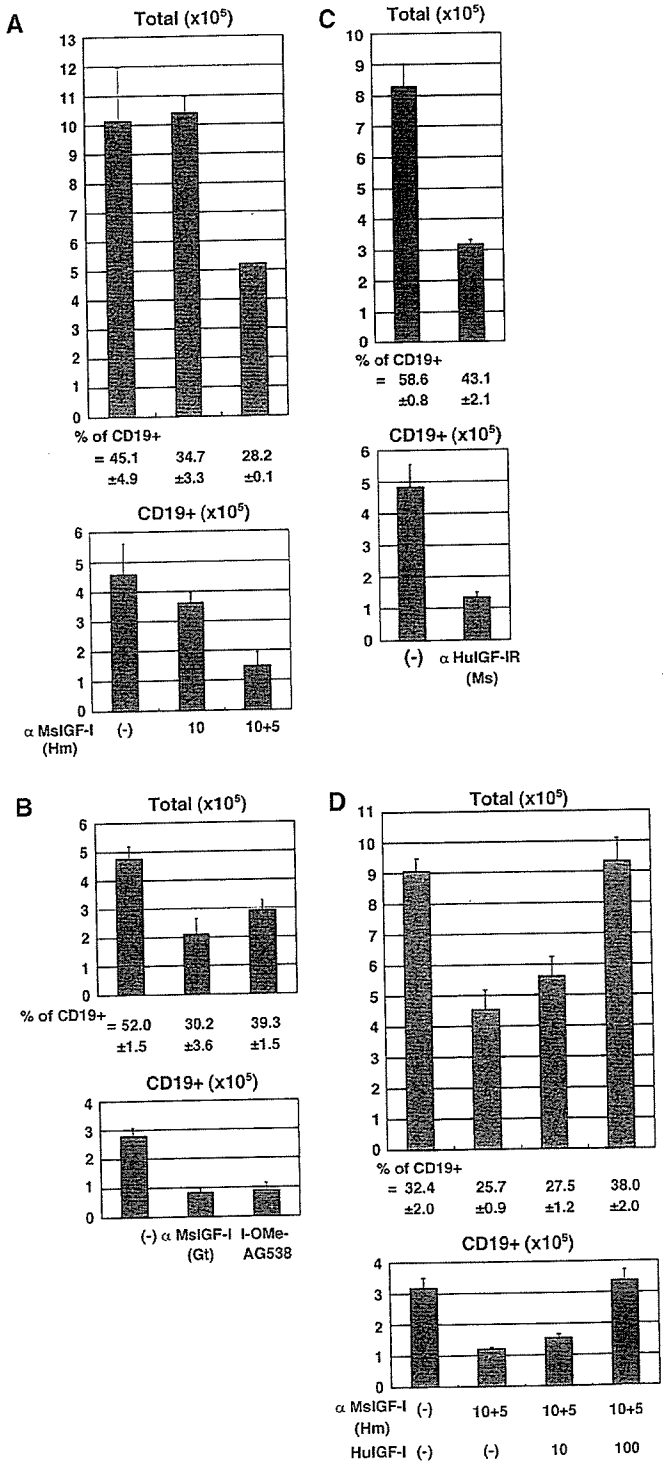

Figure 3. Effect of insulin growth factor-I (IGF-I) inhibition on human pro–B-cell development. Human bone marrow (BM) $CD34^+$ cells were cocultured with MS-5 for 4 weeks in the presence or absence of hamster anti-mouse IGF-I monoclonal antibody (mAb) [(**A**) α MsIGF-1 (Hm), either initial administration of 10 μg/mL alone (10) or a combination of an initial administration of 10 μg/mL and an additional administration of 5 μg/mL after 2 weeks of culture (10 + 5)], goat polyclonal anti-mouse IGF-I Ab [(**B**) α MsIGF-1 (Gt), 5 μg/ml)], IGF-IR kinase inhibitor I-OMe-AG538 [(**B**) 5 μM], mouse anti-human IGF-IR mAb [(**C**) α HuIGF-IR (Ms), 5 μg/mL], and a combination of α MsIGF-1 (Hm) and human IGF-I (HuIGF-1, 10, and 100 ng/mL) (**D**). Subsequent $CD19^+$ cell number was estimated using flow cytometry and is shown. Total cell number of cultured $CD34^+$ cells and the percentage of $CD19^+$ cells are also presented.

Effect of recombinant human IGFBPs on human pro–B-cell development

To assess the effect of IGFBPs on human pro–B-cell development, we challenged the present culture system with recombinant human IGFBPs. As shown in Figure 4A, of the six IGFBP members, only IGFBP-3 produced a subsequent reduction in the number of pro-B cells; the other IGFBPs did not affect human pro–B-cell development. As shown in Figure 4B, the inhibitory effect of IGFBP-3 on pro–B-cell differentiation was dose-dependent. Furthermore, IGFBP-3–mediated inhibition of $CD19^+$ cell development was cancelled by the addition of recombinant human IGF-I (Fig. 4C).

Because none of the IGFBPs other than IGFBP-3 affected pro–B-cell development from $CD34^+$ BM cells cocultured with MS-5, we tested a synergistic effect of two or more IGFBPs; no significant synergism was observed and other IGFBPs failed to enhance the effect of IGFBP3 (data not shown). Therefore, we next examined the effect of neutralization of the IGFBP function using specific Abs.

First we tested expression of IGFBPs in MS-5 cells. As shown in Figure 5A and B, RT-PCR experiments revealed that MS-5 transcribe mRNA of IGFBP-4, 5, and 6, but not 1, 2, and 3, while immunoblotting experiments using commercially available Abs detected only IGFBP-6 protein expression. Coincident with the results of immunoblotting, anti-IGFBP-2, 3, and 5 Abs did not affect MS-5–induced pro–B-cell development from $CD34^+$ BM cells (Fig. 5C). Interestingly, however, when anti-mouse IGFBP-6 Ab was added to the culture system, pro–B-cell development was significantly reduced (Fig. 5C). In addition, as shown in Figure 5D, the anti-mouse IGFBP-6 Ab–induced inhibition of pro–B-cell development was completely canceled by the addition of human IGFBP-6. In light of this data, we concluded that the IGFBP-6 produced by the MS-5 cells is essential for pro–B-cell development from $CD34^+$ BM cells.

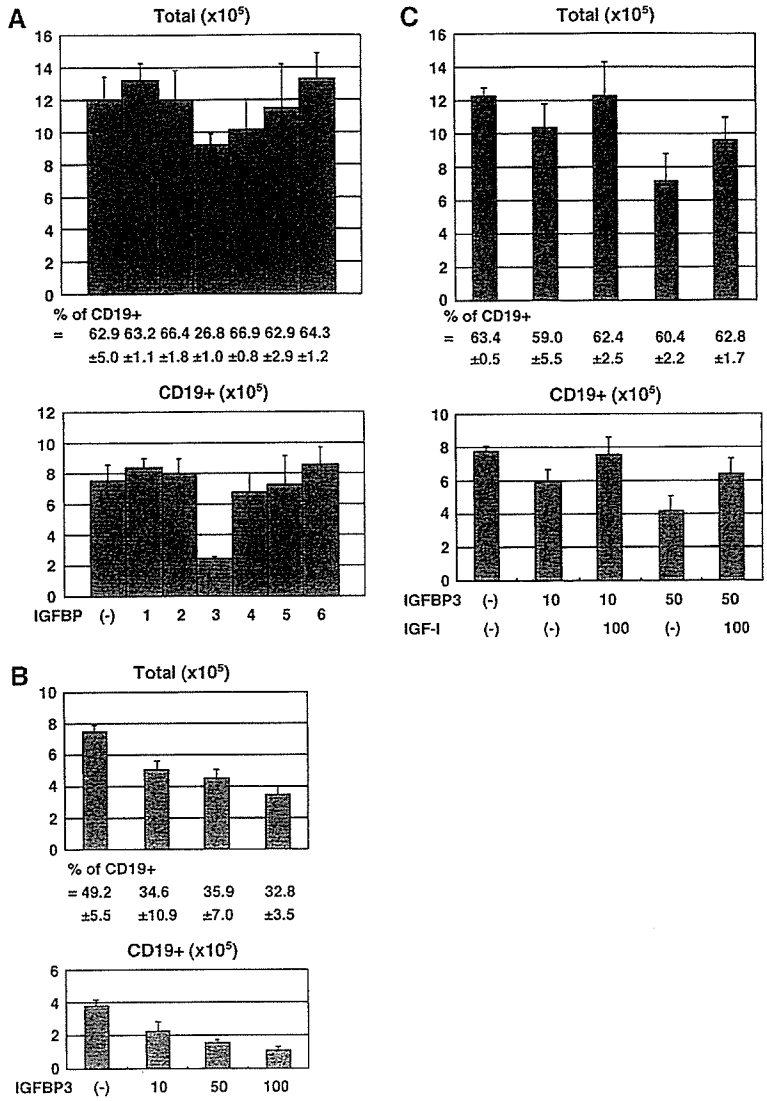

Figure 4. Effect of insulin-like growth factor (IGF)-binding proteins on human pro–B-cell development. (**A**) Human bone marrow (BM) $CD34^+$ cells were cocultured with MS-5 cells with or without 100 ng/mL each recombinant human IGF-binding proteins (IGFBP 1–6) for 4 weeks. The subsequent total cell number of cultured $CD34^+$ cells and the percentage and cell number of $CD19^+$ cells are shown. (**B**) Human BM $CD34^+$ cells were cocultured with MS-5 cells with or without different doses (ng/mL) of recombinant human IGFBP-3, as indicated, for 4 weeks and examined using the protocol described in (**A**). (**C**) Human BM $CD34^+$ cells were cocultured with MS-5 cells with or without indicated combinations of recombinant human IGFBP-3 (ng/mL) and human IGF-I (ng/mL) and examined using the protocol described in (**A**).

Discussion

In the present study, when BM $CD34^+$ cells were cultured in the presence of the murine stromal cell line MS-5, pro-B cells, but not pre-B cells, were efficiently induced. MS-5 is well known to be capable of supporting B-cell development [14–17]. However, several different groups have reported this cell line to have distinct effects on induction of B cells. Coincident with our observation, Berardi et al. [14] showed that when human HPSCs derived from umbilical CB were cultured in the presence of MS-5, $CD10^+$, $CD19^+$, and cytoplasmic μ^- pro-B cells were generated [14]. In contrast, Nishihara et al. [15] and Hirose et al. [16] reported the induction of pre-B cells from CB $CD34^+$ cells after coculturing with MS-5 in the presence of exogenous granulocyte colony-stimulating factor (G-CSF) and stem cell factor (SCF) [14–16]. Moreover, Ohkawara et al. [17] reported that surface IgM^+ mature B cells could be produced from CB $CD34^+$ cells using the same culture condition. We tested the effect of the exogenous addition of G-CSF and SCF in our culture system, but failed to observe any signs of pre–B-cell differentiation (data not shown). Although a precise reason for such a difference is unavailable, it may be possible that different stocks of MS-5 exhibit distinct effects on B-cell differentiation. A comparison of the distinct effects of different MS-5 stocks on B-cell differentiation may provide useful and interesting information.

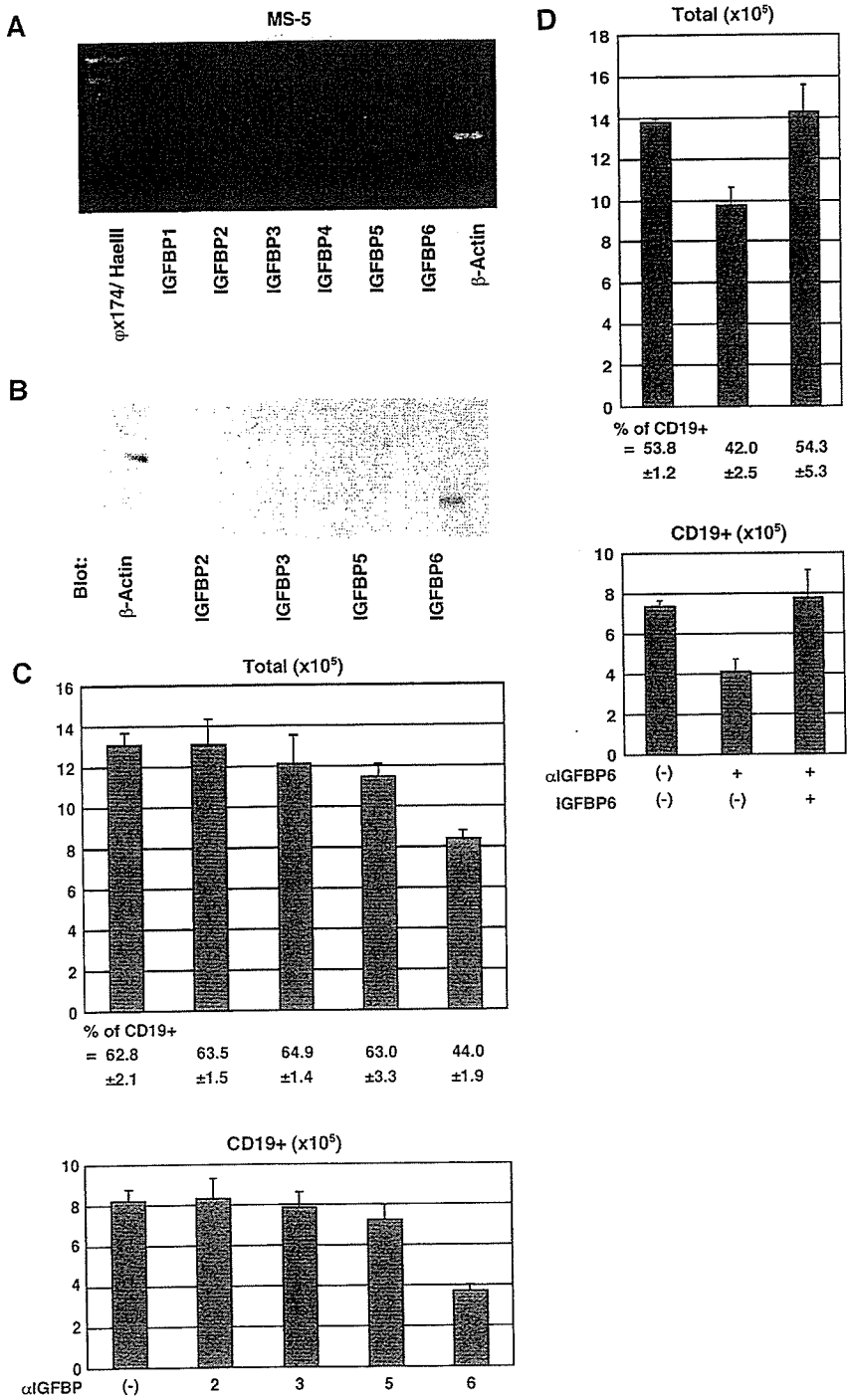

Figure 5. Effect of antibodies against insulin-like growth factor (IGF)-binding proteins on human pro–B-cell development. (**A**) Gene expression of mouse IGF-binding proteins (IGFBP) 1–6 on MS-5 cells was examined using reverse transcriptase polymerase chain reaction. As an internal control, expression of mouse β-actin was also examined. The $\phi\chi174/HaeIII$ molecular weight marker was presented in the left side. (**B**) Immunoblot analysis with goat anti-mouse IGFBP-2, 3 5, and IGFBP-6 antibodies (αIGFBP2-6, respectively) on MS-5 cell lysates was performed. (**C**) Human bone marrow (BM) $CD34^+$ cells were cocultured with MS-5 cells for 4 weeks with or without 10 μg/mL each goat antibodies against mouse IGF-binding proteins (αIGFBP), as indicated. Subsequent cell number of $CD19^+$ cells was examined using flow cytometry and is shown. Total cell number of cultured $CD34^+$ cells and percentage of $CD19^+$ cells are also presented. (**D**) Human BM $CD34^+$ cells were cocultured with MS-5 cells for 4 weeks with or without the indicated combination of αIGFBP6 (5 μg/mL) and recombinant human IGFBP-6 (100 ng/mL). Subsequent total cell number of cultured $CD34^+$ cells and percentage and cell number of $CD19^+$ cells was examined using the protocol described in (**C**).

Table 1

Name of gene	Primer sequence forward reverse	Product size (bp)
human IGF-I	5′-ACAGGTATCGTGGATGAGTG-3′ 5′-GTAACTCGTGCAGAGCAAAG-3′	263
human IGF-IR	5′-ATGTGCTGGCAGTATAACCC-3′ 5′-ACAGCCTTGGATGAACGATG-3′	929
mouse IGF-I	5′-ATGCTCTTCAGTTCGTGTGT-3′ 5′-CTTCTCCTTTGCAGCTTCGT-3′	271
mouse IGFBP-1	5′-AGATTAGCTGCAGCCCAAC -3′ 5′-TGTTCTAGGCAGCATCACTCT-3′	535
mouse IGFBP-2	5′-ATCCCCAACTGTGACAAGCA-3′ 5′-CCTCTCTAACAGAAGCAAGGGA-3′	407
mouse IGFBP-3	5′-TCCAAGTTCCATCCACTCCA-3′ 5′-GAGGCAATGTACGTCGTCTT-3′	372
mouse IGFBP-4	5′-AATTAGAGATCGGAGCAAGA-3′ 5′-TGGGAATTCCTATTGCTACA-3′	598
mouse IGFBP-5	5′-ATGAGACAGGAATCCGAACA-3′ 5′-TCAACGTTACTGCTGTCGAA-3′	269
mouse IGFBP-6	5′-TGCTAATGCTGTTGTTCGCT-3′ 5′-TGAGTGCTTCCTTGACCATC-3′	652
human GAPDH	5′-CCACCCATGGCAAATTCCATGGCA-3′ 5′-TCTAGACGGCAGGTCAGGTCCACC-3′	598
mouse Actin	5′-TGACGGGGTCACCCACACTGTGCCCATCTA-3′ 5′-CTAGAAGCATTTGCGGTGGACGATGGAGGG-3′	661

It was previously reported that earlier stages of B-cell development depend on contact with the stromal cells [15,17]. Consistently, culture supernatant of MS-5 cells failed to support pro–B-cell development from $CD34^+$ BM cells (data not shown), suggesting that cell-to-cell interaction between $CD34^+$ BM cells and MS-5 cells is essential for pro–B-cell development in our culture system. In contrast, however, we detected pro-B cells not only in adherent cell fraction, but also in floating cell fraction, while pro-B cells were more enriched in adherent cell fraction. Although contact with stromal cells should be necessary for pro-B cell development from $CD34^+$ cells, it may not always be necessary for further differentiation and/or proliferation of pro-B cells. Therefore, a portion of pro-B cells will dissociate from stromal cells and move to floating cell fraction.

As demonstrated in the present study, the MS-5 cells produced IGF-I, and elimination of IGF-I function resulted in the failure of pro–B-cell development. Previous reports have revealed that IGF-I is essential for differentiation of pro-B to pre-B cell [6,18] and expansion of B-cell population [7,8]. Therefore, our data extends previous observations and indicates that IGF-I likely plays an important role in induction of pro-B cells from HPSCs.

As we presented in Figure 2A, IGF-I is possibly secreted by a non–B-cell fraction of the cultured $CD34^+$ cells. IGF-I may also be present in the supplemented FCS. Therefore, in addition to the IGF-I secreted by MS-5 cells, IGF-I produced by a non–B-cell fraction of the cultured $CD34^+$ cells as well as that provided by supplemented FCS can also affect to pro–B-cell development. However, as we presented in Figure 2D, the biological assay has indicated that the contribution of IGF-I that may be present in the supplemented FCS can be excluded. Furthermore, because the Abs used to neutralize IGF-I activity in this study have higher specificity for mouse IGF-I than human IGF-I, it is most likely that the majority of IGF-I–mediated effects in our culture system are due to mouse IGF-I secreted by MS-5 cells.

Because IGF-I is thought to play an integrating role in hematopoiesis, it seems reasonable to consider that IGFBPs may also contribute to regulation of hematopoiesis. Evidence that IGFBPs are produced by stromal cells in the BM, yolk sac, and liver, where hematopoiesis occurs [19,20], strongly supports this notion. Indeed, a recent report by Liu et al. [21] suggested that IGFBP-3 may block differentiation of HPSCs and be capable of promoting proliferation of primitive $CD34^+CD38^-$ hematopoietic cells, contributing to expansion of the HPSC pool [21]. In this study, we further demonstrated that addition of exogenous IGFBP-3 inhibited the effect of IGF-I on pro–B-cell induction from $CD34^+$ BM cells. Although MS-5 cells do not express IGFBP-3, it has been reported that BM stromal cells produce IGFBP-3 upon stimulation with several factors, such as vitamin D3 and transforming growth factor (TGF)-β1 [22,23]. Therefore, it is conceivable that IGFBP-3 could be secreted by BM stromal cells and involved in the regulation of early hematopoiesis, including B-cell development, depending on conditions in the hematopoietic microenvironment.

As demonstrated in the present article, while all six members of the IGFBP family possess the ability to bind with IGF, only IGFBP-3 inhibited the effect of IGF-I on

pro–B-cell development. Because all other IGFBPs failed to exert synergism with the IGFBP-3 in an inhibitory effect on pro–B-cell development in our experiment (data not shown), IGFBPs may compete with each other for binding with IGF-I, and IGFBP-3 should have the highest binding affinity. Furthermore, our data indicated that IGFBP-6 is required for pro–B-cell development, and neutralization of IGFBP-6 resulted in a marked reduction in the subsequent pro–B-cell number. Therefore, it is suggested that each IGFBP can have a distinct effect on the IGF action in regulation of hematopoiesis.

Interestingly, recent reports have indicated that IGFBPs have an intrinsic ability to affect cells directly [24–29]. For example, IGFBP-2 has been shown to be mitogenic in uterine endometrial and osteosarcoma cells in the absence of IGFs [30]. IGFBP-3 has been reported to induce a reduction in cell growth, DNA synthesis inhibition, and apoptosis in specific cells in an IGF-independent manner [31–34]. Furthermore, IGFBPs have been reported to have specific cell-surface receptors; IGFBP-2 and IGFBP-3 directly bind to target cells through $\alpha5\beta1$ integrin and TGF-β type-V receptors, respectively, thereby inducing intracellular signals [35,36]. Therefore, IGFBPs might not only inhibit the effects of IGF-I during hematopoiesis, but also have intrinsic and direct bioactivities that directly affect hematopoietic cells independently of IGF-I function.

In conclusion, IGF-I and IGFBPs appear to play important roles in early B-lymphopoiesis. Although details of their molecular functions remain uncertain, IGFBPs can possibly affect hematopoietic cells in both IGF-dependent and IGF-independent manners. The present observations should contribute to a better understanding of the functional roles of IGF-I and IGFBPs in regulation of B-lymphopoiesis.

Acknowledgments

We thank S. Yamauchi for her excellent secretarial work. We also thank Dr. A. Manabe, Dr. K. J. Mori, and Dr. Y. Matsuo for gifting murine BM stromal cell line, MS-5, and human leukemia cell line HPB-NULL. This work is supported in part by MEXT. KAKENHI 16017321, JSPS. KAKENHI 17591131, the Budget for Nuclear Research of the Ministry of Education, Culture, Sports, Science and Technology, based on the screening and counseling by the Atomic Energy Commission, grant from the Japan Health Sciences Foundation for Research on Health Sciences Focusing on Drug Innovation, and a Grant for Child Health and Development from the Ministry of Health, Labour and Welfare. T. Taguchi is an Awardee of Research Resident Fellowship from the Foundation for Promotion of Cancer Research (Japan) for the 3rd Term Comprehensive 10-Years-Strategy for Cancer Control.

References

1. Clark R. The somatogenic hormones and insulin-like growth factor-1: stimulators of lymphopoiesis and immune function. Endocr Rev. 1997; 18:157–179.
2. Baxter RC. Insulin-like growth factor (IGF)-binding proteins: interactions with IGFs and intrinsic bioactivities. Am J Physiol. 2000;278: E967–E976.
3. Rajaram S, Baylink DJ, Mohan S. Insulin-like growth factor-binding proteins in serum and other biological fluids: regulation and functions. Endocr Rev. 1997;18:801–831.
4. Firth SM, Baxter RC. Cellular actions of the insulin-like growth factor binding proteins. Endocr Rev. 2002;23:824–854.
5. Kurtz A, Matter R, Eckardt KU, Zapf J. Erythropoiesis, serum erythropoietin, and serum IGF-I in rats during accelerated growth. Acta Endocrinol (Copenh). 1990;122:323–328.
6. Landreth KS, Narayanan R, Dorshkind K. Insulin-like growth factor-I regulates pro-B cell differentiation. Blood. 1992;80:1207–1212.
7. Gibson LF, Piktel D, Landreth KS. Insulin-like growth factor-1 potentiates expansion of interleukin-7-dependent pro-B cells. Blood. 1993; 82:3005–3011.
8. Jardieu P, Clark R, Mortensen D, Dorshkind K. In vivo administration of insulin-like growth factor-I stimulates primary B lymphopoiesis and enhances lymphocyte recovery after bone marrow transplantation. J Immunol. 1994;152:4320–4327.
9. Melchers F, Karasuyama H, Haasner D, et al. The surrogate light chain in B-cell development. Immunol Today. 1993;14:60–68.
10. Kiyokawa N, Kokai Y, Ishimoto K, Fujita H, Fujimoto J, Hata J. Characterization of the common acute lymphoblastic leukemia antigen (CD10) as an activation molecule on mature human B cells. Clin Exp Immunol. 1990;79:322–327.
11. Takenouchi H, Kiyokawa N, Taguchi T, et al. Shiga toxin binding to globotriaosyl ceramide induces intracellular signals that mediate cytoskeleton remodeling in human renal carcinoma-derived cells. J Cell Sci. 2004;117:3911–3922.
12. Saito M, Kiyokawa N, Taguchi T, et al. Granulocyte colony-stimulating factor directly affects human monocytes and modulates cytokine secretion. Exp Hematol. 2002;30:1115–1123.
13. Kiyokawa N, Lee EK, Karunagaran D, Lin S-Y, Hung M-C. Mitosis-specific negative regulation of epidermal growth factor receptor, triggered by a decrease in ligand binding and dimerization, can be overcome by overexpression of receptor. J Biol Chem. 1997;272: 18656–18665.
14. Berardi AC, Meffre E, Pflumio F, et al. Individual CD34+ CD38lowCD19-CD10- progenitor cells from human cord blood generate B lymphocytes and granulocytes. Blood. 1997;89:3554–3564.
15. Nishihara M, Wada Y, Ogami K, et al. A combination of stem cell factor and granulocyte colony-stimulating factor enhances the growth of human progenitor B cells supported by murine stromal cell line MS-5. Eur J Immunol. 1998;28:855–864.
16. Hirose Y, Kiyoi H, Itoh K, Kato K, Saito H, Naoe T. B-cell precursors differentiated from cord blood CD34+ cells are more immature than those derived from granulocyte colony-stimulating factor-mobilized peripheral blood CD34+ cells. Immunology. 2001;104:410–417.
17. Ohkawara JI, Ikebuchi K, Fujihara M, et al. Culture system for extensive production of CD19+IgM+ cells by human cord blood CD34+ progenitors. Leukemia. 1998;12:764–771.
18. Funk PE, Kincade PW, Witte PL. Native associations of early hematopoietic stem cells and stromal cells isolated in bone marrow cell aggregates. Blood. 1994;83:361–369.
19. Clawson TF, Lee WH, Yoder MC. Differential expression of insulin-like growth factor binding proteins in murine hematopoietic stromal cell lines. Mol Cell Endocrinol. 1996;120:59–66.
20. Abboud SL, Bethel CR, Aron DC. Secretion of insulinlike growth factor I and insulinlike growth factor-binding proteins by murine bone marrow stromal cells. J Clin Invest. 1991;88:470–475.
21. Liu LQ, Sposato M, Liu HY, et al. Functional cloning of IGFBP-3 from human microvascular endothelial cells reveals its novel role in promoting proliferation of primitive CD34+CD38- hematopoietic cells in vitro. Oncol Res. 2003;13:359–371.

22. Kveiborg M, Flyvbjerg A, Eriksen EF, Kassem M. 1,25-Dihydroxyvitamin D3 stimulates the production of insulin-like growth factor-binding proteins-2, -3 and -4 inhuman bone marrow stromal cells. Eur J Endocrinol. 2001;144:549–557.
23. Kveiborg M, Flyvbjerg A, Eriksen EF, Kassem M. Transforming growth factor-beta1 stimulates the production of insulin-like growth factor-I and insulin-like growth factor-binding protein-3 in human bone marrow stromal osteoblast progenitors. J Endocrinol. 2001; 169:549–561.
24. Valentinis B, Bhala A, DeAngelis T, Baserga R, Cohen P. The human insulin-like growth factor (IGF) binding protein-3 inhibits the growth of fibroblasts with a targeted disruption of the IGF-I receptor gene. Mol Endocrinol. 1995;9:361–367.
25. Oh Y, Muller HL, Lamson G, Rosenfeld RG. Insulin-like growth factor (IGF)-independent action of IGF-binding protein-3 in Hs578T human breast cancer cells. Cell surface binding and growth inhibition. J Biol Chem. 1993;268:14964–14971.
26. Oh Y, Muller HL, Pham H, Rosenfeld RG. Demonstration of receptors for insulin-like growth factor binding protein-3 on Hs578T human breast cancer cells. J Biol Chem. 1993;268:26045–26048.
27. Rajah R, Valentinis B, Cohen P. Insulin-like growth factor (IGF)-binding protein-3 induces apoptosis and mediates the effects of transforming growth factor-beta1 on programmed cell death through a p53- and IGF-independent mechanism. J Biol Chem. 1997;272: 12181–12188.
28. Conover CA, Bale LK, Durham SK, Powell DR. Insulin-like growth factor (IGF) binding protein-3 potentiation of IGF action is mediated through the phosphatidylinositol-3-kinase pathway and is associated with alteration in protein kinase B/AKT sensitivity. Endocrinology. 2000;141:3098–3103.
29. Rajah R, Lee KW, Cohen P. Insulin-like growth factor binding protein-3 mediates tumor necrosis factor-alpha-induced apoptosis: role of Bcl-2 phosphorylation. Cell Growth Differ. 2002;13:163–171.
30. Slootweg MC, Ohlsson C, Salles JP, de Vries CP, Netelenbos JC. Insulin-like growth factor binding proteins-2 and -3 stimulate growth hormone receptor binding and mitogenesis in rat osteosarcoma cells. Endocrinology. 1995;136:4210–4217.
31. Villaudy J, Delbe J, Blat C, Desauty G, Golde A, Harel L. An IGF binding protein is an inhibitor of FGF stimulation. J Cell Physiol. 1991;149:492–496.
32. Imbenotte J, Liu L, Desauty G, Harel L. Stimulation by TGF beta of chick embryo fibroblasts—inhibition by an IGFBP-3. Exp Cell Res. 1992;199:229–233.
33. Cohen P, Lamson G, Okajima T, Rosenfeld RG. Transfection of the human IGFBP-3 gene into Balb/c fibroblasts: a model for the cellular functions of IGFBPs. Growth Regul. 1993;3:23–26.
34. Bernard L, Babajko S, Binoux M, Ricort JM. The amino-terminal region of insulin-like growth factor binding protein-3, (1-95)IGFBP-3, induces apoptosis of MCF-7 breast carcinoma cells. Biochem Biophys Res Commun. 2002;293:55–60.
35. Schutt BS, Langkamp M, Ranke MB, Elmlinger MW. Intracellular signalling of insulin-like growth factor binding protein-2 [abstract]. Growth Horm IGF Res. 2000;0. A29.
36. Leal SM, Liu Q, Huang SS, Huang JS. The type V transforming growth factor beta receptor is the putative insulin-like growth factor-binding protein 3 receptor. J Biol Chem. 1997;272:20572–20576.

原　著

4カラーデジタルフローサイトメーターを用いた小児白血病マーカー中央診断の試み

塩沢裕介[1,2,3]，　北村紀子[1,2]，　竹野内寿美[1,2]，　田口智子[1,2]
大喜多肇[1]，　林　泰秀[4,5]，　小原　明[4,6]，　花田良二[4,7]
土田昌宏[4,8]，　藤本純一郎[1,4]，　清河信敬[1,2]

A trial of central diagnosis of childhood acute lymphoblastic leukemia with 4-color digital flow cytometer

Yusuke Shiozawa M.D., Ph.D.[1,2,3], Noriko Kitamura Ph.D.[1,2], Hisami Takenouchi Ph.D.[1,2], Tomoko Taguchi M.D., Ph.D.[1,2], Hajime Okita M.D., Ph.D.[1], Yasuhide Hayashi M.D., Ph.D.[4,5], Akira Ohara M.D., Ph.D.[4,6], Ryoji Hanada M.D., Ph.D.[4,7], Masahiro Tuchida M.D., Ph.D.[4,8], Junichiro Fujimoto M.D., Ph.D.[1,4], Nobutaka Kiyokawa M.D., Ph.D.[1,2]

[1] Department of Developmental Biology, National Research Institute for Child Health and Development
[2] Central Diagnosis Center, Tokyo Children's Cancer Study Group
[3] Department of Pediatrics, Juntendo University School of Medicine
[4] Tokyo Children's Cancer Study Group
[5] Gunma Children's Medical Center
[6] Department of Blood Transfusion, Toho University Omori Medical Center
[7] Department of Hematology and Oncology, Saitama Children's Medical Center
[8] Ibaraki Children's Hospital

Aim. We are in charge of the central diagnosis and cell preservation as a part of childhood acute lymphoblastic leukemia treatment study in Tokyo Children's Cancer Study Group. It is necessary to diagnose with a minimal quantity of specimen, to preserve leukemic cells effectively as possible. Therefore a diagnosis of childhood acute lymphoblastic leukemia by four-color analysis with digital flow cytometer has been examined.

Methods. We examined cell markers of childhood acute lymphoblastic leukemia cells by four-color analysis using digital flow cytometers. We selected the monoclonal antibodies for the diagnosis based on the recommendation of Japan Pediatric Lymphoma Study Group and made out a panel of antibodies which enable us to confirm aberrant antigen-expressions on the leukemic cells.

Results. Four colors that we used in this study were fluorescein isothyocyanate, phycoerythrin, phycoerythrin-cyanin 5.1, and phycoerythrin-cyanin 7. The most of childhood acute lymphoblastic leukemia cases could be diagnosed without CD45-gating. List mode compensation was useful to re-investigate specimens which was difficult to re-examine, because there were very few.

Discussion. Four-color analysis using digital flow cytometer is useful to save precious specimen of childhood acute lymphoblastic leukemia. We are intending to perform five-color analysis with CD45-gating as a next step.

[1] 国立成育医療センター研究所　発生・分化研究部
[2] TCCSG（東京小児がん研究グループ）　中央診断センター
[3] 順天堂大学医学部　小児科
[4] TCCSG（東京小児がん研究グループ）
[5] 群馬県立小児医療センター
[6] 東邦大学医学部大森病院　輸血部
[7] 埼玉県立小児医療センター　血液・腫瘍科
[8] 茨城県立こども病院

受付日：平成18年6月5日　受理日：平成18年6月22日

Keyword: Flow cytometry; Multi-color analysis; Childhood acute lymphoblastic leukemia.

はじめに

2004年12月より開始された東京小児がん研究グループ（Tokyo Children's Cancer Study Group, TCCSG）の小児急性リンパ芽球性白血病(Acute Lymphoblastic Leukemia, ALL)に対する多施設共同治療研究第16次案(TCCSG ALL L04-16）では，診断の施設間格差を標準化する目的で白血病の細胞マーカーの中央診断を行っている。また，余剰検体を今後の白血病研究に有効活用することを目的に，インフォームド・コンセントを得た上での細胞保存も開始された。この中央診断と細胞保存のセンターとしての役割を，国立成育医療センター研究所　発生・分化研究部が担当している。なるべく多くの細胞を保存することを優先し，かつ中央診断として充分な項目を検査するためには，必要最小限の検体量で効率的に細胞マーカー診断を行う必要がある。

そこで，われわれは，デジタルフローサイトメーター（DG-FCM）を用いた4カラー解析での細胞マーカー解析の有用性について検討した。

方　　法

白血病細胞株，健常人および小児ALL症例の血液あるいは骨髄検体に対し，fluorescein isothyocyanate (FITC)，phycoerythrin (PE)，PE-cyanin 5.1 (PC-5) またはallophycocyanin (APC)，PC-7を用いた4カラー染色を行い，DG-FCM EPICS® XL™（BECKMAN COULTER, Miami, FL）および Cytomics™ FC500 (BECKMAN COULTER) を用いて解析した。

モノクローナル抗体（monoclonal antibody, MoAb）のパネルはJapan Pediatric Lymphoma Study Group (JPLSG)“小児造血器腫瘍の免疫学的診断の標準化ワーキング・グループ”の推奨検査項目を基本に，その他有用と考えられる抗体を追加，選択した。蛍光補正を容易にするため，原則的に各組にB-lineage，T-lineage，Myeloid-lineage，と非-lineage，各1項目ずつを組み合わせ，小児で最も頻度が高いB-precursor ALLを想定して作成した（Table 1)。aberrantな抗原の発現が確認可能なMoAbの組み合わせを考慮し，minimal residual disease（MRD）検出も視野に入れた。一部の項目についてはクローンや標識の違いによる検出率の差について比較するため，複数の抗体を併用した。

Table 1

	FITC		PE		PC5		PC7	
Cell surface								
細胞表面								
1	IgG1	BC IM0639	IgG1	BC IM731585	IgG1	BC IM6607012	IgG1	BC IM6607012
2	kappa (Poly)		lamda (Poly)		CD19	DK TC051	CD45	BC IM3548
3	CD99	BD 555688	CD7	BC 6603822	CD33	BC IM2647	CD5	BC IM2642
4	CD65	BC IM1654	7.1	BC IM3454	HLA-DR	BC IM2657	CD34	BC A07509
5	CD66C	BC IM2039	CD13	BC 6602989	CD24	BC IM2645	CD2	BC IM2638
6	mue (Poly)	DK F0058	CD56	BC IM2073	CD10	BC IM2721	CD20	BC IM3629
7	gamma (Poly)	DK F0056	CD22	BC IM1835	CD15	BC IM2641	CD57	BC IM3630
8	CD49d	BC IM1404	CD18	BC IM1570	CD4	BC IM2636	CD8	BC 6607102
9	CD49e	BC IM1854	CD29	BC 6604159	CD1a	BC IM3810	CD56	BC 6607001
10	CD44	BC IM1219	CD45RA	BC IM1834	TCR-g/d	BC IM2662	CD14	BC A22331
11	CD58	BC IM1218	CD10	BC IM1915	CD38	BC IM2651	CD11c	BC 6607115
12	CD11b	BC IM0530	C42b	BC IM1447	CD244	BC IM2658	CD16	BC 6607118
13	CD184	DK RF170	Glycophorin A	BC 6607000	CD64	BC IM3855	CD41	BC 6607111
14	CD62L	BC IM1231	CD27	BC IM2578	TCR a/b	BC IM2661	CD61	BC IM3716
Cytoplasmic								
細胞質内(Pharmingen, Fix/Permを使用)								
21	IgG1	BC IM0639	IgG1	BC IM731585	IgG1	BC IM6607012	IgG1	BC IM6607012
22	TdT	DK F7139	MPO	BD 341642	CD79a	BC IM3456	CD3	BC 6607100
23	mue	BD 555782	CD179a(HSL96)					
24	Pre-BCR(HSL2)		CD22	DK R7061				

HSL2およびHSL96は、東京医科歯科大学院大学医歯学総合研究科・免疫アレルギー学分野　烏山一先生から分与いただいたものを精製、蛍光標識して用いている。
BC, Beckman Coulter社、BD, Becton Dickinson社、DK, Dako社

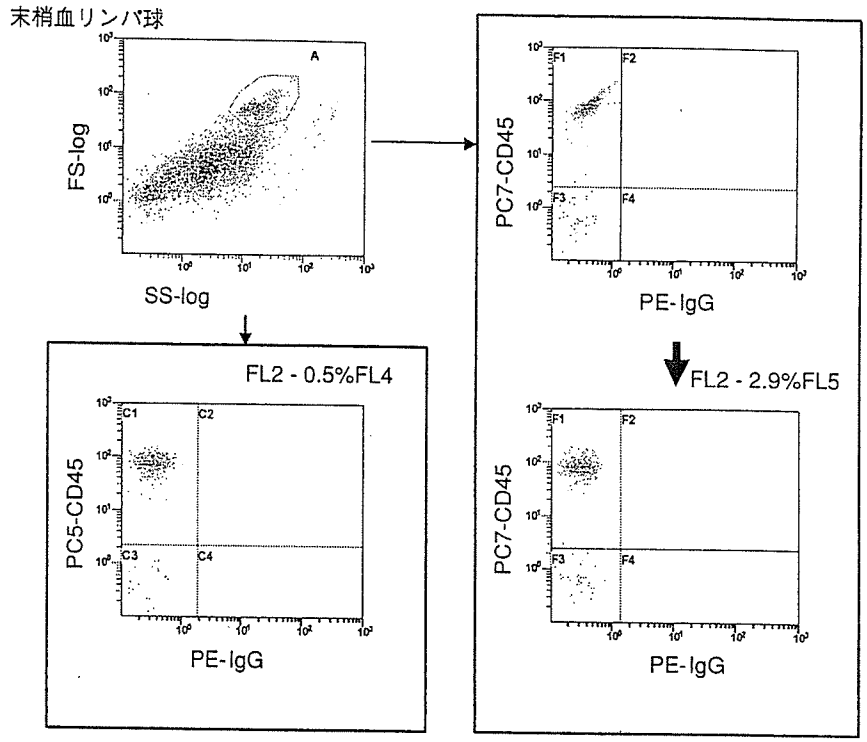

Figure 1 タンデム色素のPEチャンネルへの漏れ込み
FC500を用いて，PEをドナーとするタンデム色素，PC5とPC7のPEチャンネルへの漏れ込みについて検討した。いずれも，若干の補正が必要であった。

CD45-gatingに関しては，1）同じ検体量でなるべく多項目を検査するため，2）通常各施設の検査ではCD45-gatingを行っているのでこれと比較することが可能であること，等の理由により基本的に用いなかった。

また，診療施設から中央診断への検体の送付，余剰検体の保存については，関係各施設の倫理委員会の承認後，L04-16に登録する際に本人あるいは保護者のインフォームド・コンセントを得た上で行っている。

結　　果

染色色素の選択

PEをドナーとするタンデム色素のPEチャンネルへの漏れ込みについて，比重遠心法により分離した健常人末梢血単核球をそれぞれの蛍光色素で標識した抗CD45抗体で染色して検討した。蛍光の他のチャンネルへの漏れ込みは，測定条件やPhoto multiplier tube（PMT）の性能に大きく依存すると考えられる。今回の検討では，XLで測定した場合，現在の使用条件においては，PC-5のPEへの漏れ込みはほとんど認められなかったが，PC-7のPEへの漏れ込みは補正が必要であった。FC500で測定した場合には，PC-5のPEへの漏れ込みについても若干補正が必要であった（Figure 1）。phycoerythrin-Texas Red（ECD）は，PE以外にも，他のチャンネルへの漏れ込みが強く，抗体の組み合わせによっては，蛍光補正が難しい場合があった。

PC-5とAPCの比較を行った。CD3およびCD19について，同一クローンの抗体をそれぞれの色素で標識したもので同一の健常人末梢血単核球検体を染色し，FC500を用いて蛍光強度の比較を行ったが，PC-5とAPCでほぼ同等の蛍光強度が得られた。以上の結果に基づいて，シングルレーザーで行える簡便性からPC-5を標準的に採用し，これにFITC，PE，PC-7を加えた4色を選択した。

症例の解析

標準的な2カラー染色，あるいはCD45-gatingを加えた3カラー染色による解析ですでに診断のついている小児白血病検体を用いて，4カラー染色による染色性を比較検討した。同じ抗原に対する抗体であっても，用いるクローンによっては反応性が大きく異なる場合も想定される。しかし，同一クローンを用いた場合で

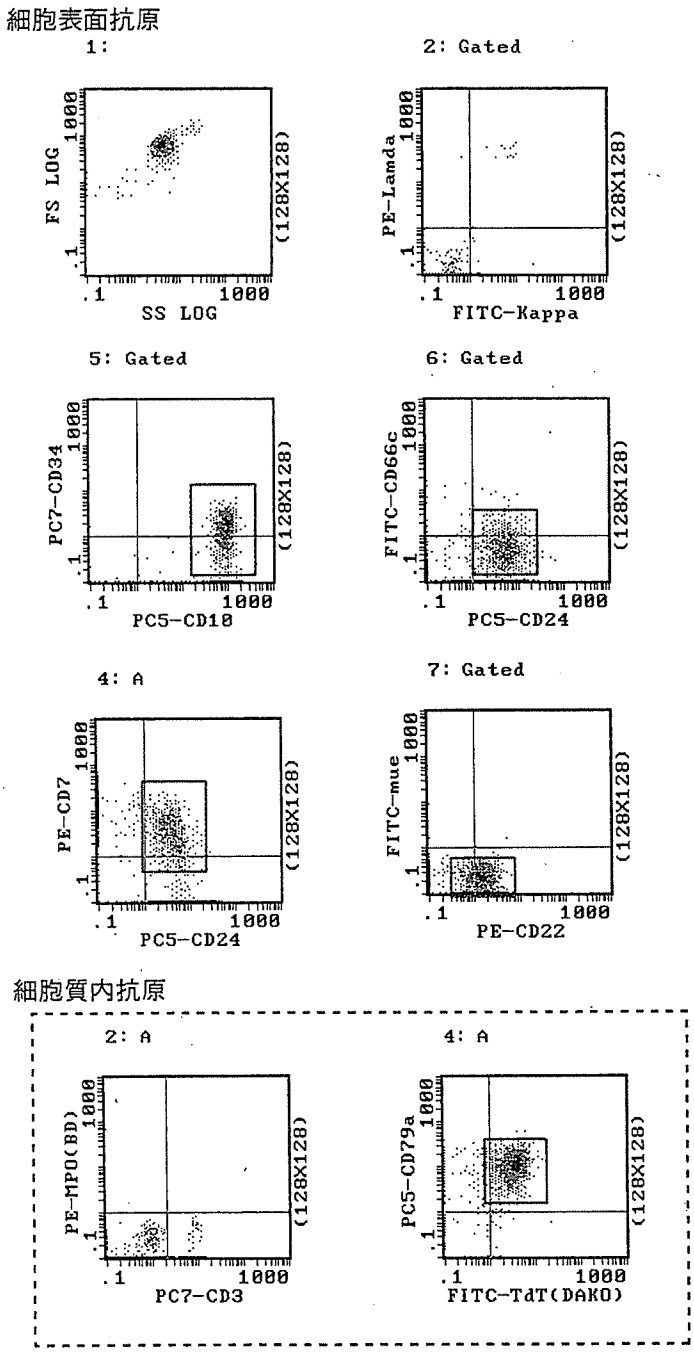

Figure 2 症例1
FS/SS-gatingで診断が容易であった，典型的なB-precursor ALL症例のマーカー結果のヒストグラムを示す。

は，標識する蛍光色素の違いによる反応性の差はほとんどの場合で認められず，標識色素の違いによる陽性/陰性の判定の不一致はなかった。

小児ALLでは，初診時検体中の芽球の割合が高い場合が比較的多いため，MoAbの組み合わせを工夫することによってCD45-gatingを行わなくても，診断に苦慮するケースは少ないと考えられた。実際にこのパネルを用いて行った解析の結果の一例をFigure 2に示す。9割以上の症例では症例1のように，芽球の割合が比較的高く，CD45-gatingを行わなくても，通常のFS/SS-gatingのみで診断可能であった（Figure 2）。しかし，一部の症例では芽球の占める割合が非常に低く，診断

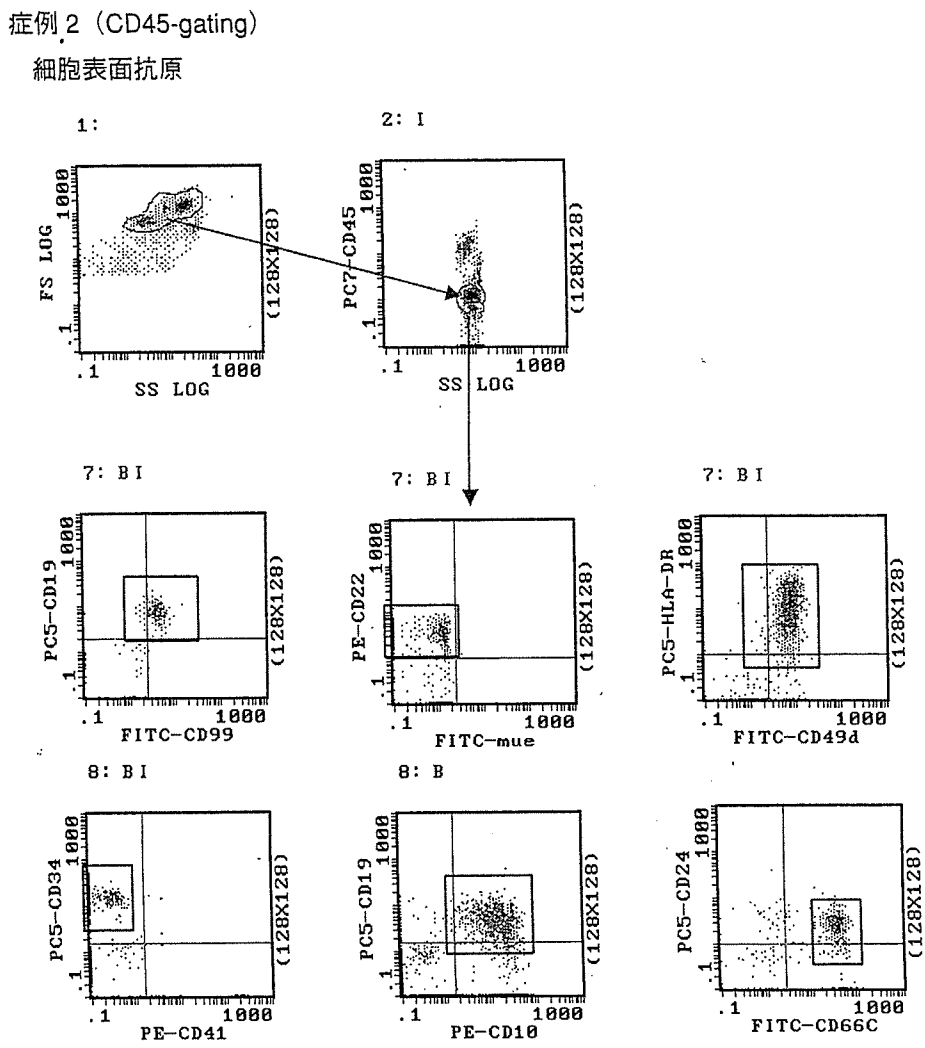

Figure 3 症例2
検体中の芽球の割合が低く，CD45-gatingが診断に有用であった，B-precursor ALL症例のマーカー結果のヒストグラムを示す。

にCD45-gatingが有用な場合も経験された（Figure 3）。

List mode data（LMD）コンペンセーションを用いた解析

FC500では，一度取得したLMDにコンピューター上でコンペンセーションをかけ直すことが可能である。検体量が少ないために再検査を行うことが困難な場合に非常に有用であった。実際に，データ取得時の蛍光補正が不充分であり，LMDコンペンセーションによって解析し直した例をFigure 4に示す。

考　察

近年の化学療法を中心とした集学的治療の進歩により，小児ALL患者の予後は70-80%以上と飛躍的に改善してきた[1]。的確な治療を開始するためには，より正確で迅速な診断が求められるようになっており，FCMによるマーカー検査は，ALLの免疫学的診断において重要な役割を担っている[2]。しかし，一方で約15%の症例が不幸な転帰をたどると言われており[3]，治療成績の一層の向上のためには，治療開始時における的確なリスク分けが必要である。そのためには，従来用いられてきた細胞マーカーや特定の染色体異常の有無などによる病型診断に加えて，治療反応性を評価するためのMRDの検索が重要であるとの報告があいついでいる。また，今後あらたな予後マーカーを捜していく上で，臨床検体を用いたトランスレーショナルリサーチが不可欠であり，そのためには診断に用いた残余細胞を効率的に保存して，より有効に研究に活用して